© 2020. Published by The Company of Biologists Ltd | Journal of Cell Science (2020) 133, jcs245415. doi:10.1242/jcs.245415

RESEARCH ARTICLE

The Na^+ pump Ena1 is a yeast epsin-specific cargo requiring its ubiquitylation and phosphorylation sites for internalization

Arpita Sen[1,*,§], Wen-Chieh Hsieh[1,‡,§], Claudia B. Hanna[1], Chuan-Chih Hsu[2], McKeith Pearson II[1], W. Andy Tao[2] and R. Claudio Aguilar[1,¶]

ABSTRACT

It is well known that in addition to its classical role in protein turnover, ubiquitylation is required for a variety of membrane protein sorting events. However, and despite substantial progress in the field, a long-standing question remains: given that all ubiquitin units are identical, how do different elements of the sorting machinery recognize their specific cargoes? Our results indicate that the yeast Na^+ pump Ena1 is an epsin (Ent1 and Ent2 in yeast)-specific cargo and that its internalization requires K^{1090}, which likely undergoes Art3-dependent ubiquitylation. In addition, an Ena1 serine and threonine (ST)-rich patch, proposed to be targeted for phosphorylation by casein kinases, was also required for its uptake. Interestingly, our data suggest that this phosphorylation was not needed for cargo ubiquitylation. Furthermore, epsin-mediated internalization of Ena1 required a specific spatial organization of the ST patch with respect to K^{1090} within the cytoplasmic tail of the pump. We hypothesize that ubiquitylation and phosphorylation of Ena1 are required for epsin-mediated internalization.

KEY WORDS: Endocytosis, Internalization, Ena1, Epsin, Ubiquitin, Phosphorylation

INTRODUCTION

Endocytosis is a vital cellular process required for multiple cellular functions including nutrient uptake and control of cell membrane composition. This process involves the selective retention of cargo proteins into nascent endocytic sites by the endocytic machinery through the recognition of sequence-encoded motifs or post-translationally added tags.

In addition to its classical role in proteosome-mediated protein degradation, ubiquitin (Ub) plays an important role as a post-translational tag for protein sorting into different subcellular compartments. Indeed, the Ub tag mediates membrane protein internalization and targeting to the lysosomal/vacuolar and recycling compartments (reviewed in Mukhopadhyay and Riezman, 2007; Traub and Lukacs, 2007).

Since Ub constitutes the main trafficking signal in *Saccharomyces cerevisiae* (reviewed in Lauwers et al., 2010), studies in yeast have been instrumental in advancing our understanding of the mechanisms operating in Ub-mediated sorting. For example, it has been clearly established that budding yeast utilizes the E3 ubiquitin ligase Rsp5 to promote cargo ubiquitylation relevant to endocytosis and other vesicle trafficking events (Belgareh-Touze et al., 2008; Lauwers et al., 2010). Indeed, Rsp5-mediated ubiquitylation is required for the internalization of cargoes such as the pheromone receptor Ste2 (Dunn and Hicke, 2001; Hicke and Riezman, 1996), the uracil transporter Fur4 (Galan et al., 1996), the general amino acid permease Gap1 (Soetens et al., 2001) and the zinc transporter Zrt1 (Gitan and Eide, 2000) among others. Although Rsp5 is capable of directly interacting with PPxY motif-containing substrates via its WW domains (McNatt et al., 2007; Oestreich et al., 2007; Stawiecka-Mirota et al., 2007; Sullivan et al., 2007a), this consensus sequence is not present in all cargoes that undergo Ub-dependent trafficking (Belgareh-Touze et al., 2008; Polo and Di Fiore, 2008). In those cases, the PPxY motif-containing, arrestin-related trafficking (ART) adaptor family specifically bridges cargo proteins to Rsp5 (Alvaro et al., 2014; Becuwe et al., 2012; Lin et al., 2008; Nikko and Pelham, 2009; Nikko et al., 2008; Prosser et al., 2015).

Following ubiquitylation, plasma membrane cargoes are recognized by endocytic adaptors, such as epsin (Ent1 and Ent2 in yeast) and Eps15 (or Ede1 in *S. cerevisiae*), which contain ubiquitin-binding elements like the Ub-interacting motifs (UIMs) or Ub-associated (UBA) domains. As a consequence of these interactions, cargo is incorporated into nascent endocytic sites and trafficked towards degradative vacuolar/lysosomal compartments or recycling routes.

Specifically, Eps15 is known to be responsible for the internalization of the AMPA receptor (Lin and Man, 2014) and Cx43 (Girão et al., 2009) among other ubiquitylated cargoes; while epsin is involved in the uptake of vascular endothelial growth factor receptor 2 (VEGFR2) (Pasula et al., 2012), notch ligands (Overstreet et al., 2004; Tian et al., 2004; Wang and Struhl, 2004, 2005) and the epithelial sodium channel ENaC (Staruschenko et al., 2005; Wang et al., 2006).

The different relevance of these adaptors for the internalization of various ubiquitylated cargoes highlights a crucial knowledge gap in the field: how do identical ubiquitin units attached to different cargoes mediate specific, but differential recognition by Ub-binding proteins? (which in turn is crucial to promote the needed trafficking outcomes).

Here, we report the identification of the Na^+ pump Ena1 (Exitus Natru 1) as the first described yeast epsin-specific cargo. Further, we established that the internalization of this cargo required K^{1090} and integrity of UIMs in epsin.

Importantly, our results suggest that epsin-mediated internalization of Ena1 requires two independent post-translational events –

[1]Department of Biological Sciences, Purdue University, West Lafayette, IN 47907, USA. [2]Department of Biochemistry, Purdue University, West Lafayette, IN 47907, USA.
*Present address: Aromyx Inc., 319 N. Bernardo Avenue, Mountain View, CA 94043, USA. ‡Present address: Section on Cellular Communication, National Institute of Child Health and Human Development, National Institutes of Health, Bethesda, MD 20892, USA.
§These authors contributed equally to this work
¶Author for correspondence (Claudio@purdue.edu)

R.C.A., 0000-0001-5623-0073

Handling Editor: David Stephens
Received 19 February 2020; Accepted 14 July 2020

Journal of Cell Science (2020) 133, jcs245415. doi:10.1242/jcs.245415

phosphorylation of an upstream Ser/Thr-rich motif and ubiquitylation in the cytoplasmic domain of the transporter. Epsin co-immunoprecipitated with an Ena1 mutant that emulated constitutive phosphorylation and ubiquitylation.

In summary, our results indicate that the yeast endocytic adaptor epsin likely acts upon its cargo based on the presence of a phosphorylated Ser/Thr motif upstream of a ubiquitylated lysine residue. We speculate that other Ub-binding elements of the sorting system (such as Ede1) also use coincidence detection of determinants (likely different from the ones recognized by epsins) to identify their targets among multiple ubiquitylated cargoes.

RESULTS

The yeast Na^+ pump Ena1 is internalized in an epsin-dependent manner

S. cerevisiae is known to use Ub as its main sorting tag and has been instrumental to study the function of endocytic adaptors (Lauwers et al., 2010). Therefore, we relied on this organism to investigate the mechanism by which epsin recognizes its specific targets among multiple ubiquitinated-cargoes. However, it was first necessary to identify a yeast membrane protein that would substantially rely on this adaptor for its internalization.

In contrast to mammals, yeast does not have homologs for established epsin-specific cargoes such as Notch-ligands and VEGFR2-like receptor tyrosine-kinases. Although ENaC-sodium channel homologs are not present either, *S. cerevisiae* has sodium pumps, such as those of the Ena protein family. Pumps and channels are evolutionarily/mechanistically related (Artigas and Gadsby, 2002; Gadsby, 2009) and their plasma membrane levels have been shown to be controlled by Ub-mediated endocytosis (Helenius et al., 2010; Lecuona et al., 2007). Therefore, we speculated that members of the Ena family (Ena1–Ena5) were suitable candidates to be internalized in an epsin-dependent manner.

Given its relevance among family members (Garciadeblas et al., 1993; Haro et al., 1991; Wieland et al., 1995), we focused our studies on the Ena1 paralog (also known as Pmr2) using an *ENA1::GFP* construct under the control of the *MET25* methionine-repressible promoter (Logg et al., 2008; Wadskog et al., 2006). The stability of wild-type (WT) and mutated versions of Ena1–GFP was verified by western blotting, while also monitoring their cellular distribution pattern in comparison to free GFP and ER-retained transmembrane proteins (Fig. S1).

In agreement with previous observations (Logg et al., 2008; Wadskog et al., 2006), we observed that, in WT cells, Ena1 partitioned between the plasma membrane and intracellular compartments (Fig. 1A). Furthermore, more than 95% of Ena1–GFP intracellular structures were stained by the lipophilic dye FM4-64 (following a 30 min chase), indicating that they are connected to the endocytic pathway (Fig. S2).

We quantified the internal (I) GFP fluorescence intensity as a fraction of the total (T) fluorescence intensity (denoted I/T) and defined an 'intracellular localization' ('IL') index as the cumulative fraction of cells with more than 50% of Ena1 in intracellular compartments (see Materials and Methods). WT cells exhibited an 'IL' of 0.89±0.04 (mean±s.e.m., Fig. 1A) indicating that ∼89% of this cell population contained Ena1 enriched (>50%) in internal compartments. In addition, individual WT cells showed Ena1–GFP localized at the plasma membrane (P), corresponding to only 13% of their total fluorescence intensity [to give a fraction (P/T) of median value 0.13 P/T; Fig. 1B]. The evaluation of cell-based observations (P/T) along with the quantitative, population-based IL index is important to avoid result misinterpretation due to variability of individual cell images. See Materials and Methods and Fig. S3 for a more detailed description of IL and P/T value estimation and their complementary meaning.

As expected for proteins undergoing endocytosis, Ena1 accumulated at the plasma membrane of the general endocytosis-deficient *sla2*Δ strain and therefore cells had a median amount of Ena1–GFP localized at the plasma membrane double that of WT cells (Fig. 1B) while exhibiting an IL=0.08±0.04 (Fig. 1A). As described previously (Roth and Davis, 1996), internalization of the constitutively endocytosed pheromone receptor Ste3 was also substantially inhibited in *sla2*Δ as compared to WT cells (Fig. 1A,B).

If as hypothesized, Ena1 internalization was dependent on epsin function, then the transporter should be largely localized at the plasma membrane (i.e. should display low IL and high P/T values) in *ent1*Δ*ent2*Δ double epsin deleted cells (hereafter referred to as ΔΔ). Indeed, as opposed to the WT strain, only ∼11% of the ΔΔ cells had Ena1 enriched in internal compartments (IL=0.11±0.05; Fig. 1A). Similar to *sla2*Δ, ΔΔ cells showed a substantial accumulation of Ena1–GFP at the plasma membrane (Fig. 1B). In contrast, as expected for a cargo that does not depend on the epsins for internalization (Maldonado-Báez et al., 2008), Ste3 was properly localized to internal structures in 100% of ΔΔ cells (Fig. 1A). Importantly, re-introduction of either yeast epsin Ent1 or Ent2 could rescue the Ena1 localization defect in ΔΔ cells (Fig. 1C). Along the same lines, Ena1 localization to intracellular compartments was not affected in either single epsin knockout (*ent1*Δ or *ent2*Δ), also suggesting that the epsins are redundant for promoting Ena1 uptake (Fig. 1C).

Further supporting the epsin specificity of Ena1 internalization, the transporter distribution was not affected by deletion of the genes corresponding to the Yap180 family of endocytic adaptors (Fig. S4A).

Although the Ena1–GFP distribution phenotype in ΔΔ cells was identical to the one seen in the classical endocytosis-defective strain *sla2*Δ (Fig. 1), a direct observation of Ena1 internalization defects in epsin-deficient cells was lacking. Therefore, based on previous knowledge, we devised a strategy to directly test the presence of Ena1 endocytosis abnormalities in ΔΔ cells. It is known that under salt stress conditions Ena1 expression is induced and the protein is translocated to the plasma membrane to promote Na^+ efflux (Ruiz and Ariño, 2007; Serrano et al., 1999; Yenush, 2016). Furthermore, Ena1 has been proposed to undergo internalization (Logg et al., 2008) and vacuolar degradation (Wadskog et al., 2006). Therefore, we speculated that upon salt stress relief, Ena1 will be subjected to internalization mediated by epsins followed by vacuolar degradation, and that this process will be affected in ΔΔ cells.

To test the potential contribution of epsins to low salt-induced downregulation of Ena1, we designed a salt stress relief assay (see Materials and Methods). Briefly, WT and ΔΔ cells were subjected to salt stress (0.5 M NaCl) following a short induction of Ena1–GFP expression. This was done to ensure that the expressed Ena1–GFP was recruited to and maintained at the plasma membrane to enable the efflux of excess Na^+. Under Ena1 expression-suppressed conditions, and after lowering the salt concentration in the medium, cells were imaged over time and the peripherally localized fluorescence intensity of Ena1–GFP was quantified at each time-point. Fig. 2A shows a representative experiment where at least 50 cells at each time point were analyzed. In WT cells, the peripheral fluorescence intensity of Ena1–GFP underwent a sharp decrease 45 min after salt excess removal, indicating transporter uptake (Fig. 2A, upper panel). At later time points, the vacuolar fluorescence also dramatically diminished, indicating Ena1–GFP

Journal of Cell Science (2020) 133, jcs245415. doi:10.1242/jcs.245415

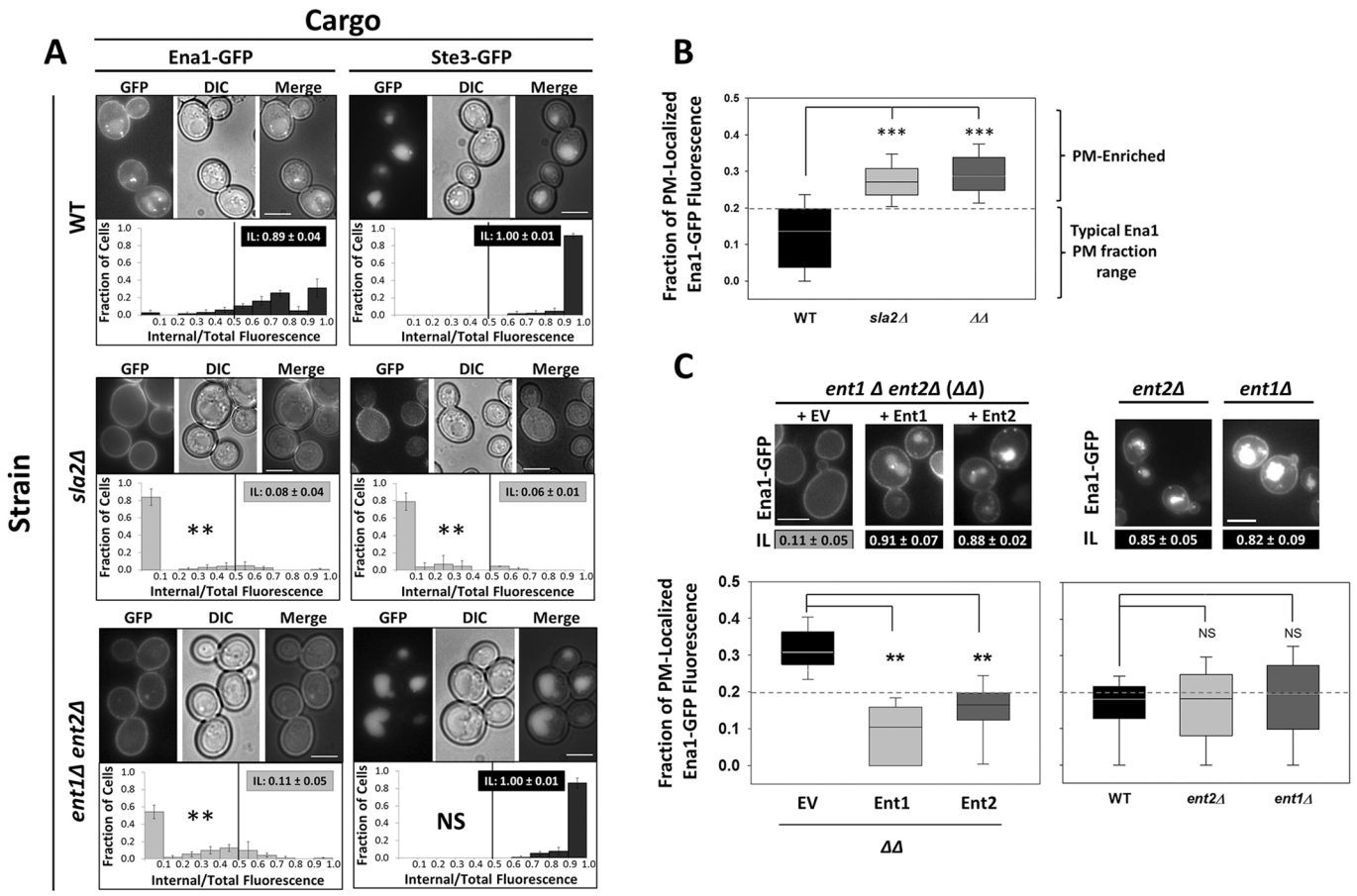

Fig. 1. The cellular distribution of Ena1–GFP depends on epsin. (A) Localization of Ena1–GFP and Ste3–GFP in wild type (WT), *sla2*Δ or *ent1*Δ*ent2*Δ (ΔΔ) cells. Representative images show the cellular distribution of the indicated GFP-tagged cargoes (GFP), differential interference contrast (DIC) and merged channels. Quantification of GFP-fusion protein intracellular localization over 90 cells was performed as described in the Materials and Methods. Results are shown as fraction of cells vs Internal/Total fluorescence histograms; the Kolmogorov–Smirnov test (with a Bonferroni-corrected α for multiple comparisons α_C<0.05/2=0.025) was used to statistically analyze the difference between the distribution of Ena1-GFP (or Ste3-GFP) in WT versus *sla2*Δ and ΔΔ cells: $^{**}P<\alpha_C$; NS, not significant. 'Intracellular Localization' (IL) index values (calculated over at least three histograms; mean±s.e.m.) shown in gray boxes were significantly different from the corresponding WT IL (using the Student's *t*-test with an $\alpha=\alpha_C$). (B) Relative Ena1–GFP plasma membrane (PM) accumulation in WT, *sla2*Δ or ΔΔ cells. The fraction of PM-localized Ena1–GFP fluorescence with respect to the total fluorescence (P/T; see Materials and Methods) in the indicated cell backgrounds are shown as box plots. The statistical significance of differences between the non-normally distributed P/T values for Ena1–GFP in WT vs *sla2*Δ or ΔΔ cells was estimated by using the Wilcoxon's test with an $\alpha=\alpha_C$. $^{***}P\ll\alpha_C$. (C) Localization and relative Ena1–GFP PM accumulation in cells expressing no epsin or a single paralog. The values of IL and P/T were estimated for Ena1–GFP expressed in ΔΔ cells transformed with empty vector (EV, no epsin present), or with single-copy plasmids carrying either epsin paralog gene from their endogenous promoter; as well as for Ena1–GFP expressed in epsin single KOs (*ent2*Δ and *ent1*Δ: expressing only Ent1 and Ent2, respectively) cells. Representative images are shown. For box plots, the box represents the 25–75th percentiles, and the median is indicated. The whiskers show the minimum and maximum with outliers and negative numbers excluded. $^{**}P$<0.05; NS, not significant. Scale bars: 5 µm.

degradation (Fig. 2A, upper panel). In striking contrast, the fluorescence intensity of GFP–Ena1 at the periphery of ΔΔ cells remained at high values over time (Fig. 2A, lower panel), indicating that epsins are required for efficient Ena1–GFP removal from the plasma membrane.

The role of epsins in Ena1–GFP retrieval from the plasma membrane was confirmed in complementary experiments using flow cytometry. Specifically, WT and ΔΔ cells were allowed to express Ena1–GFP overnight, and samples were analyzed by flow cytometry at 0 h and 5 h under Ena1–GFP expression-suppressed conditions. Fig. 2B shows that 5 h after turning off the *MET25* promoter (with 2 mM methionine) fluorescence intensity associated with WT cells was low due to internalization and vacuolar degradation of GFP–Ena1, whereas at 5 h, ΔΔ cells displayed high fluorescence intensity closer to that seen at the 0 h time point. It should be noted that, despite other endocytic adaptors (e.g. Ede1) being present, Ena1 was severely impaired for uptake in ΔΔ cells.

These results indicate that in the absence of epsins, internalization of Ena1 triggered by salt stress relief is substantially delayed. Also, as a whole, these experiments support the conclusion that changes in Ena1 cellular distribution (e.g. Fig. 1, and all throughout this study) upon deletion of the PM-localized epsin endocytic adaptors, largely reflects impairment in the Na^+-transporter uptake.

Ena1 internalization requires the UIMs in epsin and Ena1 K^{1090}

Since ubiquitylation has been implicated in the trafficking of Ena1 (Wadskog et al., 2006) and epsin is a known Ub-binding protein, we hypothesized that the UIMs of epsin would be required for Ena1 internalization. Indeed, we observed that Ent1/2 variants bearing mutations that abolish the functionality of the two epsin UIMs [Ent1/2^{Um}: Ent1$^{S177D,\ S201D}$ and Ent2$^{S187D,\ S218D}$ (Aguilar et al., 2003)] were unable to rescue the Ena1 internalization defect seen in ΔΔ cells (Fig. 3).

Journal of Cell Science (2020) 133, jcs245415. doi:10.1242/jcs.245415

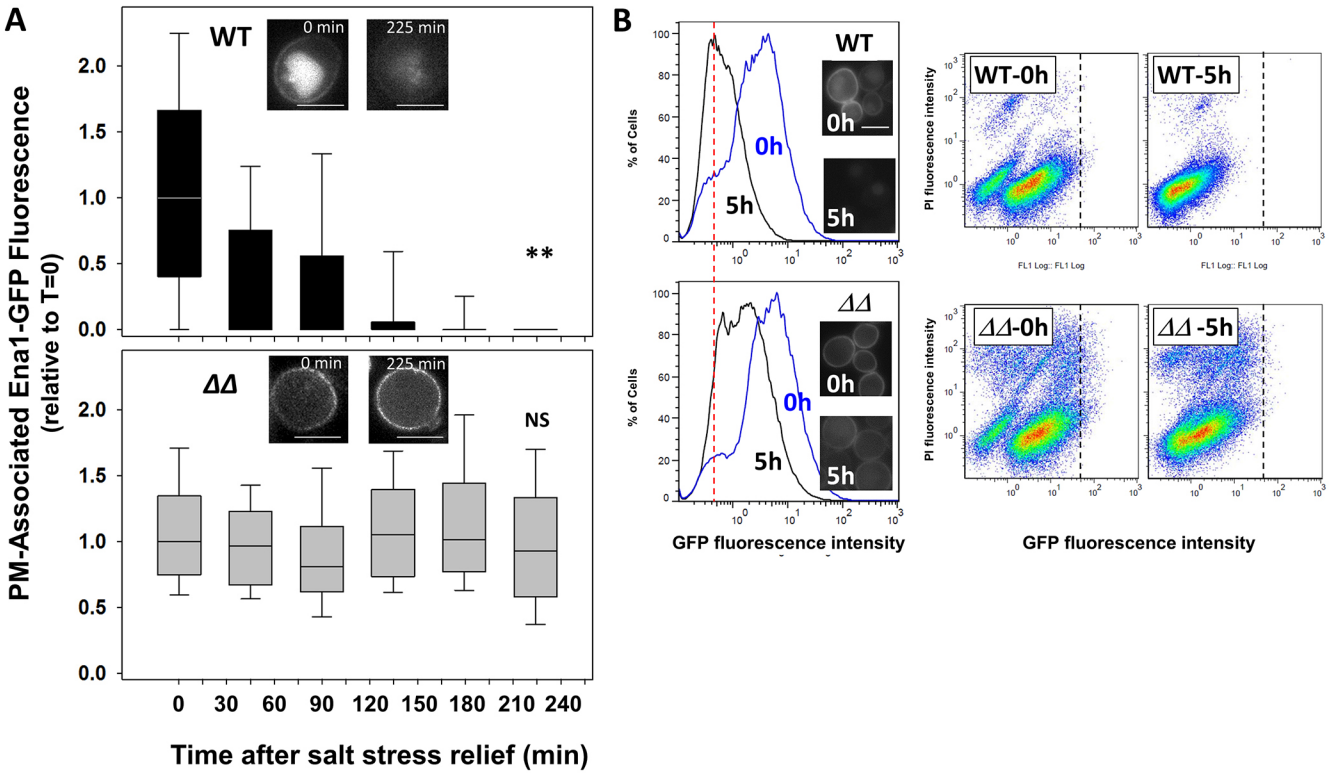

Fig. 2. Ena1 internalization is epsin dependent. (A) Salt stress relief stimulates Ena1 internalization in WT, but not ΔΔ cells. PM-associated fluorescent intensity of Ena1–GFP following salt stress-relief was tracked over time. A representative experiment shows PM fluorescence intensity relative to time 0 of >30 cells per time-point. Statistical significance of the difference between the PM-associated fluorescent intensity of Ena1–GFP at time 0 and 225 min for WT and ΔΔ cells was assessed. ***P*<0.01; NS, not significant (Wilcoxon's test). Representative images for the indicated time points and for each strain are shown. Scale bars: 5 µm. See Materials and Methods for details. For box plots, the box represents the 25–75th percentiles, and the median is indicated. The whiskers show the minimum and maximum with outliers and negative numbers excluded. (B) Removal of Ena1–GFP from the PM is delayed in ΔΔ cells with respect to WT. Total fluorescence intensity of Ena1–GFP from 5×10^4 cells was measured by flow cytometry at 0 and 5 h after production of Ena1–GFP was halted. The percentage of cells vs GFP fluorescence intensity histograms are shown for WT (upper left) and ΔΔ (lower left) cells at 0 (blue trace) and 5 h (black trace). Red vertical dashed line marks the peak position of Ena1–GFP fluorescence intensity in WT cells after 5 h chase; note that the corresponding 5 h peak for ΔΔ cells is shifted to the right (higher fluorescence intensity). Representative images of the analyzed cells are shown as insets. Scale bar: 10 µm. The corresponding propidium iodide (PI) vs GFP fluorescence intensity scatter plots are included (right). Black vertical dashed lines define the GFP fluorescence intensity boundaries at time 0 for WT and ΔΔ cells. Note the marked decrease in fluorescence intensity for WT as compared to ΔΔ cells after 5 h chase. See Materials and Methods for details.

In agreement with these findings, the UIM-containing C-termini of Ent1 or Ent2 (ΔENTH fragments), but not their lipid-binding ENTH domains, were also sufficient to suppress Ena1 uptake deficiency in ΔΔ cells (Fig. 3). It is worth reiterating that although ΔΔ cells express other Ub-binding endocytic adaptors such as Ede1, Ena1 uptake showed a strong dependence on epsin UIM integrity.

K^{1090} is necessary for Ena1 internalization

Since epsin UIMs are required for Ena1 internalization, we hypothesized that this cargo will undergo lysine-ubiquitylation as a requisite for endocytosis. It should be noted that Ena1 is a relatively large (1091 residues) protein with ten predicted transmembrane regions and a large number of cytosol-facing lysine residues as potential targets for ubiquitylation. In order to tackle the daunting task of identifying putative internalization-relevant ubiquitylation sites, we took into consideration pioneering findings from other authors working with yeast multi-spanning endocytic cargoes. Specifically, it has been determined that the internalization of the a-factor receptor Ste3, and the α-factor receptor Ste2, required ubiquitylation of their cytosolic C-termini (Hicke and Riezman, 1996; Rohrer et al., 1993; Roth and Davis, 2000; Roth et al., 1998). Based on these findings, we hypothesized that the Ena1 C-terminal tail (residues 1044–1091) is important for its uptake. In agreement with this, C-terminal truncations of Ena1 displayed intracellular distribution defects (Fig. 4A,B). Furthermore, an Ena1 truncation that lacked only the last four amino acids GIKQ ($Ena1^{\Delta1088\text{-}1091}$) failed to internalize in WT cells (Fig. 4A,B). Since lysine residues are sites for ubiquitylation, we speculated that K^{1090} was the residue within the GIKQ sequence responsible for Ena1 internalization. In fact, the $Ena1^{K1090R}$ mutant was severely impaired for uptake, thereby indicating a requirement of K1090 for Ena1 internalization (Fig. 4C). Point mutations of the adjacent residues ($Ena1^{G1088A}$, $Ena1^{I1089A}$ and $Ena1^{Q1091A}$) did not grossly affect the localization of the transporter (although the Q1091A mutant showed a slight accumulation of Ena1 at the PM) (Fig. 4C).

Importantly, an in-frame C-terminal fusion of ubiquitin with the $Ena1^{K1090R}$ mutant was able to re-establish its intracellular localization (Fig. 4C), suggesting that K^{1090} was a target for ubiquitylation.

Furthermore, and despite challenges for detecting notoriously difficult targets such as mono-ubiquitylated products and for pulling down multi-pass transmembrane proteins like Ena1, we found that Ena1 WT, but not a K1090R mutant (lacking the proposed ubiquitylation site) could be affinity-captured using Ub-binding beads (Fig. 4D). The data also suggest that, from all possible ubiquitylation sites, K^{1090} is an important target, as mutation of this

Journal of Cell Science (2020) 133, jcs245415. doi:10.1242/jcs.245415

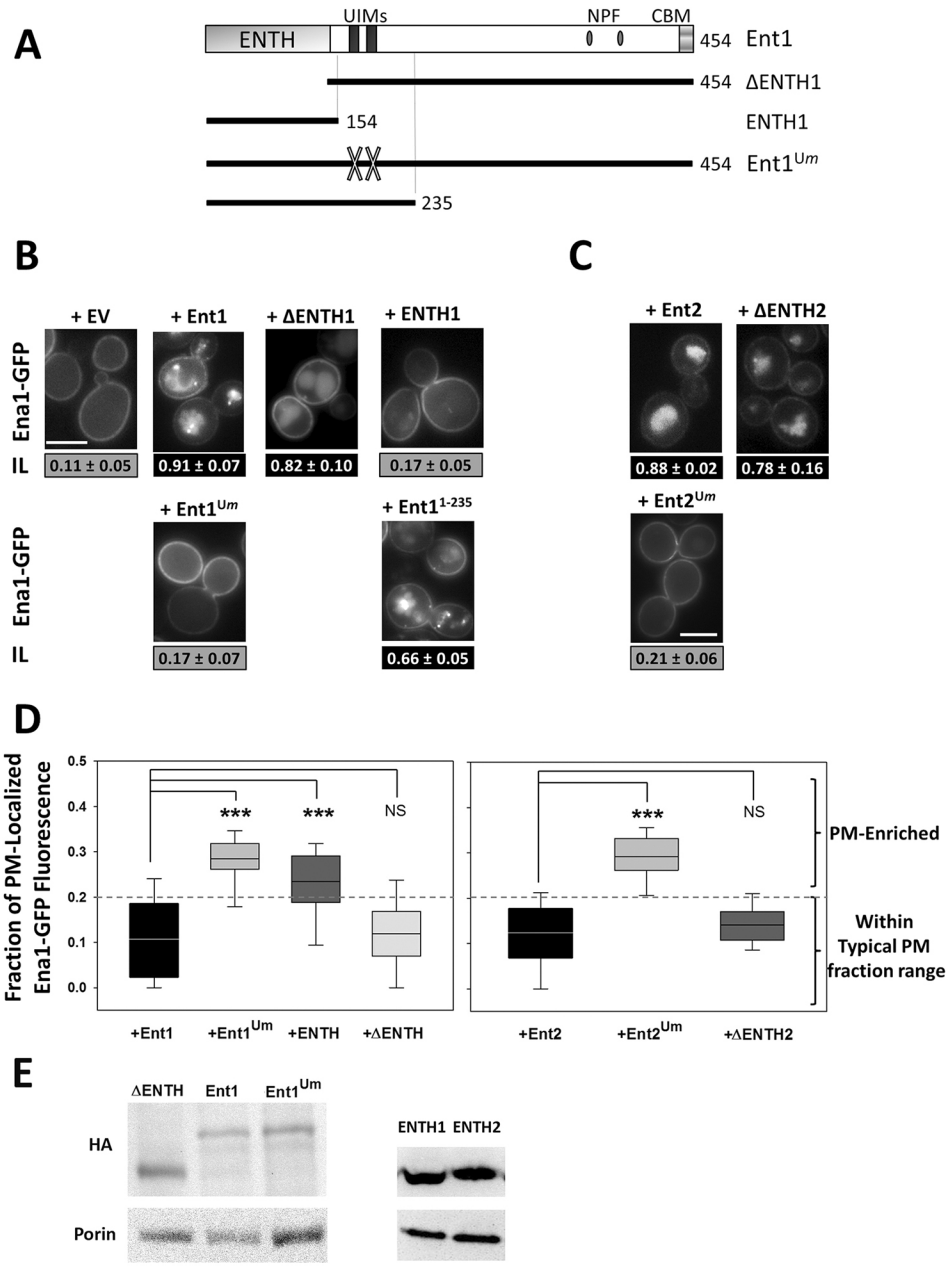

Fig. 3. The UIMs in epsin are required to sustain Ena1 internalization. (A) ΔΔ cells were transformed with empty vector (EV) or plasmids encoding for different Ent1 or Ent2 variants listed. ENTH, Epsin N-terminal homology (domain); NPF, Asn (N)-Pro (P)-Phe (F) tripeptide; CBM: clathrin-binding motif; $Ent1^{Um}$, Ent1 UIM mutant ($Ent1^{S177D,\ S201D}$); $Ent2^{Um}$, Ent2 UIM mutant. (B,C) Representative images and internalization indexes for cells with Ent1 (B) and Ent2 (C) WT and mutated variants are shown. Scale bars: 5 µm. Image analysis and quantification was performed as described in Fig. 1A. IL values shown in black boxes are statistically different from ΔΔ+EV (Bonferroni corrected α_C<0.05/5=0.01). (D) Ena1–GFP relative PM accumulation values for cells expressing the indicated Ent1 or Ent2 mutants as sole source of epsin were represented and statistically analyzed with respect to Ent1 or Ent2 as in Fig. 1B. ***P<αC=0.01; NS, not significant. (E) Western blotting was conducted as described in the Materials and Methods on whole-cell lysates from cells expressing the indicated proteins. Presence of epsin-related variants was investigated using an anti-HA antibody, while the signal from the mitochondrial protein porin was used as loading control.

residue led to no detectable signal (Fig. 4D). Among other causes, this could be because a putative Ub unit introduced at K^{1090} is target for sequential di-ubiquitylation (and/or higher-order modification).

Ub fusion in-frame to $Ena1^{K1090R}$ was used as a positive control (100% of Ena1 molecules were 'ubiquitylated'). This $Ena1^{K1090R}$–Ub construction was efficiently affinity captured; however, differences in band intensity between mono- and di/multi-Ub product suggest that in-frame fusion of Ub was perhaps less efficiently targeted for Ub-linkage than Ena1 WT. In summary, Ena1 undergoes ubiquitylation and K1090 (a residue required for its endocytosis) plays an important role in such process.

Experiments performed with *rcy1*Δ (recycling-deficient) strain showed that none of these mutant proteins accumulated in the characteristic/aberrant endosomal compartment of this strain suggesting the absence of mistrafficking to recycling routes (Fig. S4B). To test whether in-frame fusion of Ub to $Ena1^{K1090R}$ was steering this mutated protein from the Golgi complex directly to the vacuole rather than restoring its uptake, we compared the intracellular fluorescent signal of $Ena1^{K1090R}$ variants fused to GFP with the signal from the same proteins tagged with pHluorin (Fig. S4C). pHluorin is a GFP variant unable to emit fluorescence in low pH environments; therefore, the fluorescence signal produced by any Ena1–pHluorin fusions are expected to be more intense at the plasma membrane (if the protein indeed reaches the cell surface) where the pH is out of the quenching range. On the one hand, Fig. S4C shows that $Ena1^{K1090R}$ accumulates at the plasma membrane and therefore no difference is seen when this protein is labeled with GFP or pHluorin. On the other hand, $Ena1^{K1090R}$–Ub fused to GFP shows a signal in the vacuole that is substantially more intense than in any other compartment, while the pHluorin fusion (which is dimmed in more acidic organelles like the vacuole) showed a weak signal that was mostly restricted to the plasma membrane (as expected for an efficiently internalized cargo; Fig. S4C). Furthermore, absence of the epsins (*ent1/2*; i.e. the ΔΔ strain) caused the pHluorin–$Ena1^{K1090R}$–Ub fusion to strongly accumulate at the cell cortex (Fig. S4C). These results strongly support the idea

Journal of Cell Science (2020) 133, jcs245415. doi:10.1242/jcs.245415

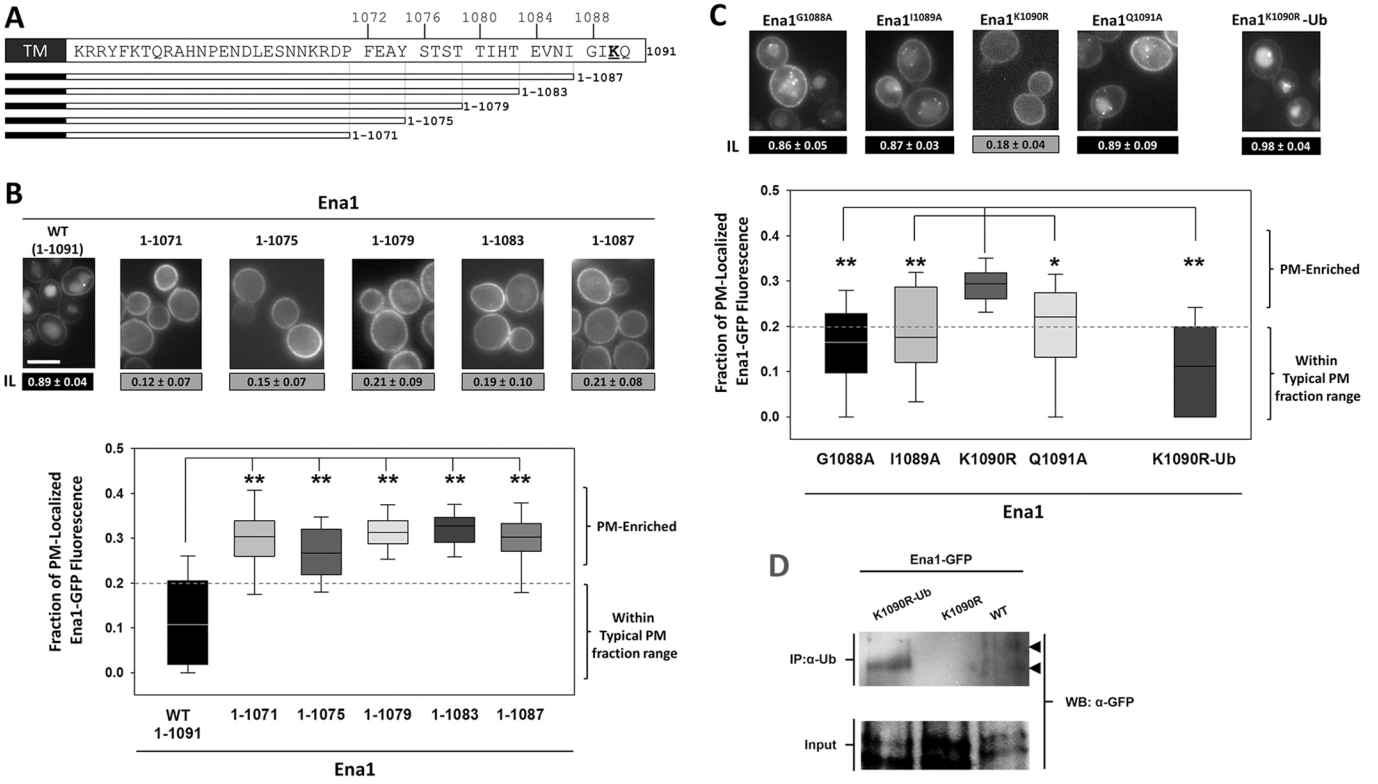

Fig. 4. Ena1 K^{1090} is necessary for the transporter internalization. The indicated Ena1–GFP truncations (A,B) and point mutants (C,D) were expressed in yeast cells. IL indexes and relative PM accumulation values (B,C) were estimated as in Fig. 1. Representative images are included. Scale bar for B and C: 5 µm. Differences between $Ena1^{1-1091}$ (WT full-length) and truncations (B) or between $Ena1^{K1090R}$ and other point mutants or $Ena1^{K1090R}$–Ub (C) were statistically analyzed as described in Materials and Methods and in Fig. 1 (*P<0.05; **$P \ll \alpha_C$=0.01). (D) Affinity-capture of Ub-proteins was performed as described in the Materials and Methods. Ena1–GFP proteins were detected by western blotting with an anti-GFP antibody. Arrowheads point to ubiquitylated Ena1 species. Box plots in B and C exclude negative values, as described in Fig. 1.

that $Ena1^{K1090R}$–Ub reaches the plasma membrane from where it is internalized towards the vacuole in an epsin-dependent manner.

Ena1 internalization depends on Art3

Rsp5 is an E3 ubiquitin ligase in yeast involved in internalization of cargo, which can directly interact with its substrates via its WW domains (Lauwers et al., 2010). However, many cargoes do not contain the PPxY motif required for interacting with the WW domains of Rsp5 (Belgareh-Touze et al., 2008). Nevertheless, it is very well established that the arrestin-related trafficking (ART) family of adaptors specifically recognizes cargoes and they recruit Rsp5 to mediate selective cargo ubiquitylation via their own PPxY motif (Becuwe et al., 2012; Lauwers et al., 2010). Since Ena1 does not contain a PPxY motif, we tested whether its uptake was ART dependent. We quantified Ena1 localization within a panel of single ART-deleted cells (from *art1*Δ through *art10*Δ; Fig. S5). While Ena1 uptake was normal in most of these strains, it was significantly affected in *art3*Δ (Fig. 5A,C) and partially in *art6*Δ cells (Fig. S5). It should be noted that Art3 and Art6 are paralogs, and while the double Art3/6 deletion showed significant abnormalities in Ena1 distribution, this was not substantially worse than *art3*Δ (Fig. S5). This result suggests that although Art6 contributes to Ena1 internalization, Art3 is the major player in this process. Importantly, and as expected, this defect could be bypassed by an in frame fusion with Ub (Fig. 5A,C). We also monitored the uptake of transferrin receptor-like protein 1 (Tre1), which is a PPxY motif-containing protein that undergoes Rsp5-dependent ubiquitylation in an Art-independent manner (Stimpson et al., 2006; Sullivan et al., 2007). As predicted, Tre1 internalization was not affected in *art3*Δ cells (Fig. 5A). Importantly, expressing Art3 from a plasmid in *art3*Δ cells re-established Ena1–GFP internalization (Fig. 5B,C).

Interestingly, Ena1 uptake was also partially affected by deletion of the Art3 paralog Art6, but not by knoukout of Art9 (Fig. S5). Since Art9 has been shown to be involved in Ena1 functional regulation (Marqués et al., 2015), but our data showed that is dispensable for internalization, we speculate that this Art protein might play a role in a different Ena1 trafficking event or other regulatory step.

In summary our results indicate that Ena1 is ubiquitylated (Fig. 4D) and its internalization is impaired by: (1) epsin deletion or epsin UIM mutation (rescued by re-expression of either Ent1 or Ent2 or their corresponding UIM-containing C-terminal fragments); (2) mutation of the C-terminal Ena1 K1090R (rescued by a C-terminal Ub fusion-in-frame); or (3) deletion of the Ub-ligase Rsp5 adaptor Art3 (rescued by a C-terminal Ub fusion-in-frame). Therefore, we speculate that yeast epsins (via their UIMs) recognize Ena1 ubiquitylated (by an Art3–Rsp5 complex) at K^{1090}.

In addition to K^{1090}, a S/T-rich region within the Ena1 C-terminus is necessary for its internalization

Although our results strongly suggest that Ena1 ubiquitylation is necessary for UIM-mediated recognition by epsin, other ubiquitylated yeast cargoes (e.g. Ste3) are internalized independently of Ent1 and Ent2. A corollary observation (further emphasizing Ub-binding adaptor specificity) is that, even in the presence of other ubiquitin-binding endocytic proteins (e.g. Ede1), Ena1 uptake is severely

Journal of Cell Science (2020) 133, jcs245415. doi:10.1242/jcs.245415

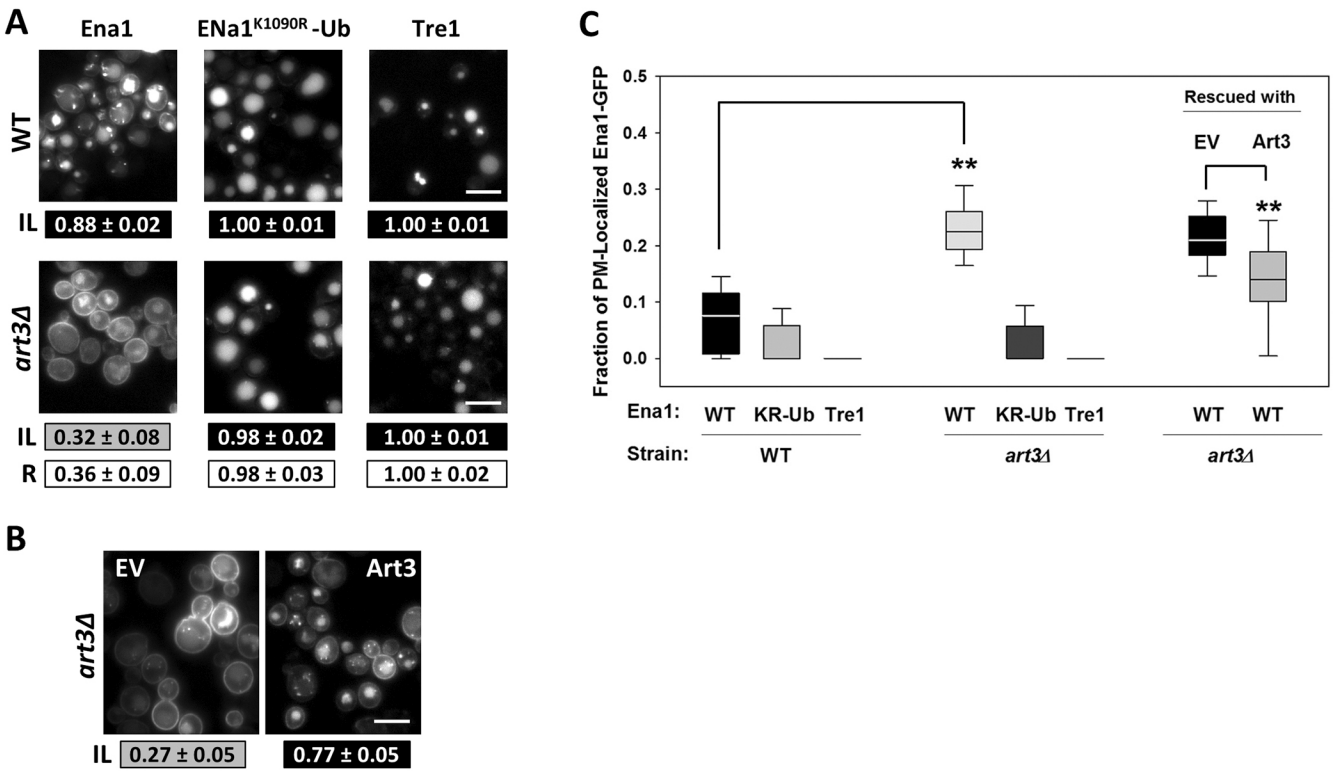

Fig. 5. Ena1 internalization is Art3 dependent. (A) Intracellular localization of Ena1–GFP, Ena1^{K1090R}–Ub–GFP and Tre1–GFP was analyzed in WT and *art3*Δ cells. IL indexes were estimated and analyzed as described in Fig. 1. Representative images are included. Values in white boxes represent the ratio between the corresponding ILs for each protein in *art3*Δ and WT cells. (B) Ena1–GFP-expressing *art3*Δ cells were transformed with empty vector (EV) or plasmid for expression of Art3. Cells were imaged and analyzed as described in the Materials and Methods. (C) Relative PM accumulation for the indicated Ena1 mutants was estimated and statistically analyzed with respect to the corresponding WT strain or EV-transformed *art3*Δ as in Fig. 1. $^{**}P \ll \alpha = 0.05$–Wilcoxon's test. KR-Ub: Ena1^{K1090R}-Ub. Box plots exclude negative values, as described in Fig. 1. Scale bars: 10 µm.

affected by the absence of epsins. Therefore, this led us to a very important unanswered question in the field: given that all Ub units are identical, what is the basis for cargo (e.g. Ena1) specificity for different adaptors (e.g. epsin)?

We speculated that a detection of an ubiquitylated lysine residue at the same time as another putative Ena1 determinant leads to epsin specificity. Since the C-terminus of Ena1 holds one of these elements (K^{1090}), we started our search for a hypothetical Ub-independent determinant within this region. Specifically, we performed a scanning mutational analysis of the Ena1 C-terminal tail by simultaneous mutation of four consecutive amino acids to glycine (denoted Gly ×4 mutants) (Fig. 6). This approach was preferred to alanine scanning to avoid the introduction of a potentially hydrophobic stretch of four alanine residues. It should also be highlighted that point mutations or truncations introduced between residues 1050–1070 in Ena1 C-terminus led to ER retention (see example in Fig. S1).

As expected, mutation of the $G^{1088}IKQ^{1091}$ sequence led to loss of Ena1 internalization by elimination of the critical K^{1090} (Fig. 6A,B). While most Gly ×4 Ena1 mutants displayed normal endocytosis, mutation of the $S^{1076}TST^{1079}$ residues caused a substantial impairment of cargo uptake (Fig. 6A,B). Interestingly, although 90% of cells expressing the $T^{1080}IHT^{1083}$-to-GGGG Ena1 mutant showed enrichment of the transporter in intracellular structures (Fig. 6A), they exhibited a PM-associated GFP fluorescence fraction slightly above normal levels (Fig. 6B). Therefore, we speculate that the threonine residues included in this region are functionally linked to the $S^{1076}TST^{1079}$ patch. The identified S/T-rich (including T^{1080}) sequence constituted an obvious candidate for phosphorylation. Indeed, mutational analysis and detection of the corresponding phosphorylated peptides by mass spectrometry indicated this to be the case (see below).

Ena1 C-terminal ST patch mutational analysis

Mutation of $S^{1076}TST^{1079}$ to TSTS did not affect Ena1 uptake (Fig. 6C,D), suggesting that, rather than the exact sequence, the biochemical nature of S/T residues (e.g. as targets for phosphorylation) is important for its role in Ena1 internalization. Next, we changed the glycine residues in the uptake-defective $G^{1076}GGG^{1079}$ (Ena1^{G1076GGG1079}=Ena1^{GGGG}) quadruple mutant to aspartate (one at a time or in pairs) to mimic constitutive phosphorylation and to assess the relative importance of the residues within this ST patch. While single mutants failed, a double aspartate mutation (Ena1$^{G1076D,\ G1077D}$; denoted Ena1^{DDGG}) rescued the uptake of Ena1 (Fig. 6C). All other double aspartate mutations showed some level of improvement (Fig. 6C); that is, a slight increase of the number of cells with the corresponding Ena1–GFP mutant enriched in intracellular compartments and a decrease in levels of the transporter at the PM as compared to Ena1^{GGGG} (except for the GDDG mutant, Fig. 6C). However, only the Ena1–GFP DDGG and GGDD mutants also showed median P/T values within the normal range for the transporter (Fig. 6C). Since only Ena1^{DDGG} exhibited all signs of substantial rescue (i.e. significant increase in IL values and significant decrease in PM-associated mutant Ena1–GFP levels compatible with the normal range for the transporter), we concluded that the first two positions within the ST patch substantially contribute to Ena1 uptake.

To complement these studies, we generated S/T-to-alanine mutations of the ST motif in Ena1^{WT} to mimic constitutive dephosphorylation.

Journal of Cell Science (2020) 133, jcs245415. doi:10.1242/jcs.245415

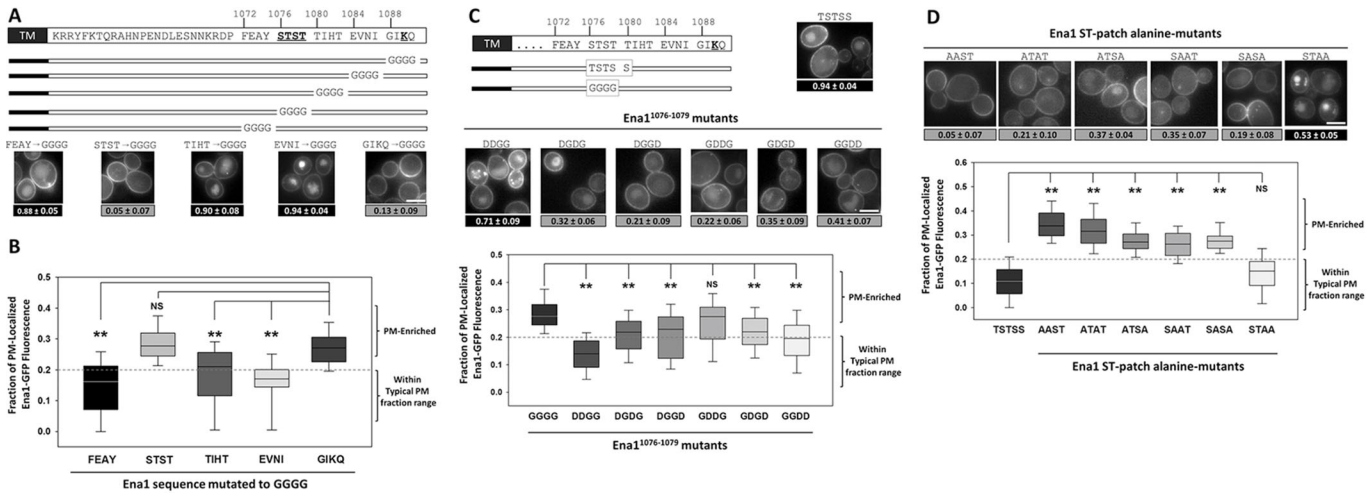

Fig. 6. Ena1 S^{1076} T^{1077} residues are required for its internalization and targeted for phosphorylation. The indicated Ena1–GFP mutants were expressed in yeast cells and IL indexes and relative PM accumulation values were estimated as in Fig. 1. Representative images are included. Scale bars: 5 µm. Differences between samples were statistically analyzed as described in Materials and Methods and in Fig. 1 (**$P \ll \alpha_C$=0.008); NS, not significant. Box plots exclude negative values, as described in Fig. 1.

While all Ena1 S/T mutants displayed defective uptake at certain extent, $Ena1^{S1076A\ T1077A}$ ($Ena1^{AAST}$) was the most affected (Fig. 6D). In addition, the sole presence of S^{1076} and T^{1077} was enough to maintain proper Ena1–GFP uptake ($Ena1^{STAA}$–GFP; Fig. 6D).

As a whole, these results strongly suggest that the ST motif is a target for phosphorylation, and also suggest that in terms of function, S^{1076} and T^{1077} are the most relevant residues.

Ena1 internalization depends on Yck1/2

In order to gain insight as to what kinases could target the ST patch for phosphorylation, we monitored Ena1 distribution in seven strains bearing deletions in genes encoding for different S/T kinases (*yck1-Δ1::ura3, yck2-2ts; ypk1*Δ; *ypk2*Δ; *pkh1*Δ; *pkh2*Δ; *ptk2*Δ and *kkq8*Δ). Specifically, we selected strains deficient in S/T kinases implicated in salt homeostasis and/or endocytosis. While most of them did not lead to Ena1 uptake abnormalities, a yeast casein kinase-1 (Yck1) knockout and Yck2 temperature-sensitive double mutant strain (*yck1-Δ1::ura3, yck2-2ts*; hereafter referred to as yck^{ts}) was significantly affected in Ena1 internalization at the restrictive temperature of 37°C (Fig. 7A). Although this result suggests that Yck function is required for the transporter uptake, it should be noted that given the widespread function of Yck1/2 in endocytosis (Feng and Davis, 2000; Hicke et al., 1998; Marchal et al., 2002, 2000; Panek et al., 1997), yck^{ts} cells show general endocytosis defects and an overall decreased fitness (even at permissive temperatures). Importantly, we reasoned that if the Yck proteins are directly involved in Ena1 phosphorylation at the ST patch, and this is required for uptake, then the $Ena1^{S1076D,\ T1077D}$ ($Ena1^{DDST}$) mutant that emulates constitutive phosphorylation of part of the ST patch, should be able to bypass the requirement for Yck1/2-mediated phosphorylation. Indeed, in contrast to $Ena1^{WT}$, $Ena1^{DDST}$ was able to significantly internalize in yck^{ts} cells even at the restrictive temperature (Fig. 7B). Furthermore, *in vitro* phosphorylation assays showed that His_6-tagged Yck1/2 proteins (purified from yeast lysates) were capable of phosphorylating the bacterially produced purified $Ena1^{K1090R}$–Ub CT (where CT refers to C-terminal fragment, i.e. $Ena1^{1076\text{-}1091}$; Fig. 7C).

It should be noted that as a whole, the ST patch of Ena1 is flanked by the putative casein kinase phosphorylation sites $E^{1073}AYS^{1076}$ and $T^{1083}E$. Indeed, both S^{1076} and T^{1083} were found to be phosphorylated in whole-cell lysates of ΔΔ cells expressing Ena1–GFP and Yck1/2 by mass spectrometry (Table S1). These phosphorylated S/T residues are expected to yield additional casein kinase phosphorylation sites, for example: $pS^{1076}TS^{1078}$ and $T^{1080}IHpT^{1083}$ (where pS or pT represent phosphorylated serine or threonine, respectively), which could further propagate the post-translational modification within the ST patch. These sites were also found to be phosphorylated using mass spectrometry (Table S1). This propagation mechanism is expected to continue further and to yield a highly phosphorylated ST patch.

To further confirm the relevance of casein kinases for the internalization of Ena1, we also tested the effect of Yck1/2 overexpression on the uptake of an endocytosis-defective mutant (Fig. 7D). We reasoned that if Yck enzymes were involved in inducing Ena1 internalization, then their overexpression should enhance the transporter uptake. Since endocytosis of WT Ena1–GFP is highly efficient (IL≥0.8; P/T of ∼0.13) with a small window for improvement, we selected a transporter mutant with IL<0.5 and P/T>0.13 to improve the experiment sensitivity. Specifically, we chose the partial phosphorylation $S^{1076}A$ Ena1 mutant ($Ena1^{ATST}$), which should be less efficient at initiating Yck-sequential phosphorylation of the ST patch. We predicted that Yck overexpression would ameliorate such phosphorylation impairment, improving the Ena1 mutant uptake. Indeed, overexpression of either Yck1 or Yck2 led to an increase in the proportion of cells with substantial intracellular $Ena1^{ATST}$–GFP and decreased the median accumulation of the mutant at the plasma membrane (Fig. 7D).

In summary, this section shows that Ena1 internalization is impaired by mutation of the $S^{1076}TST^{1079}$ patch to glycine or alanine (but this defect was reduced by introduction of asparate residues in positions 1076 and 1077). This ST patch is flanked by putative casein kinase phosphorylation sites and phosphorylation of this region was verified by mass spectrometry of yeast lysates. Interestingly, overexpression of Yck1/2 improved the uptake of an Ena1 ST patch partial mutant (S1076A). Ena1 internalization is also impaired upon Yck1/2 lack-of-function (but this defect could be bypassed by emulation of constitutive phosphorylation using the $Ena1^{S1076D,\ T1077D}$ mutant). Furthermore, Yck1 or Yck2 purified

Journal of Cell Science (2020) 133, jcs245415. doi:10.1242/jcs.245415

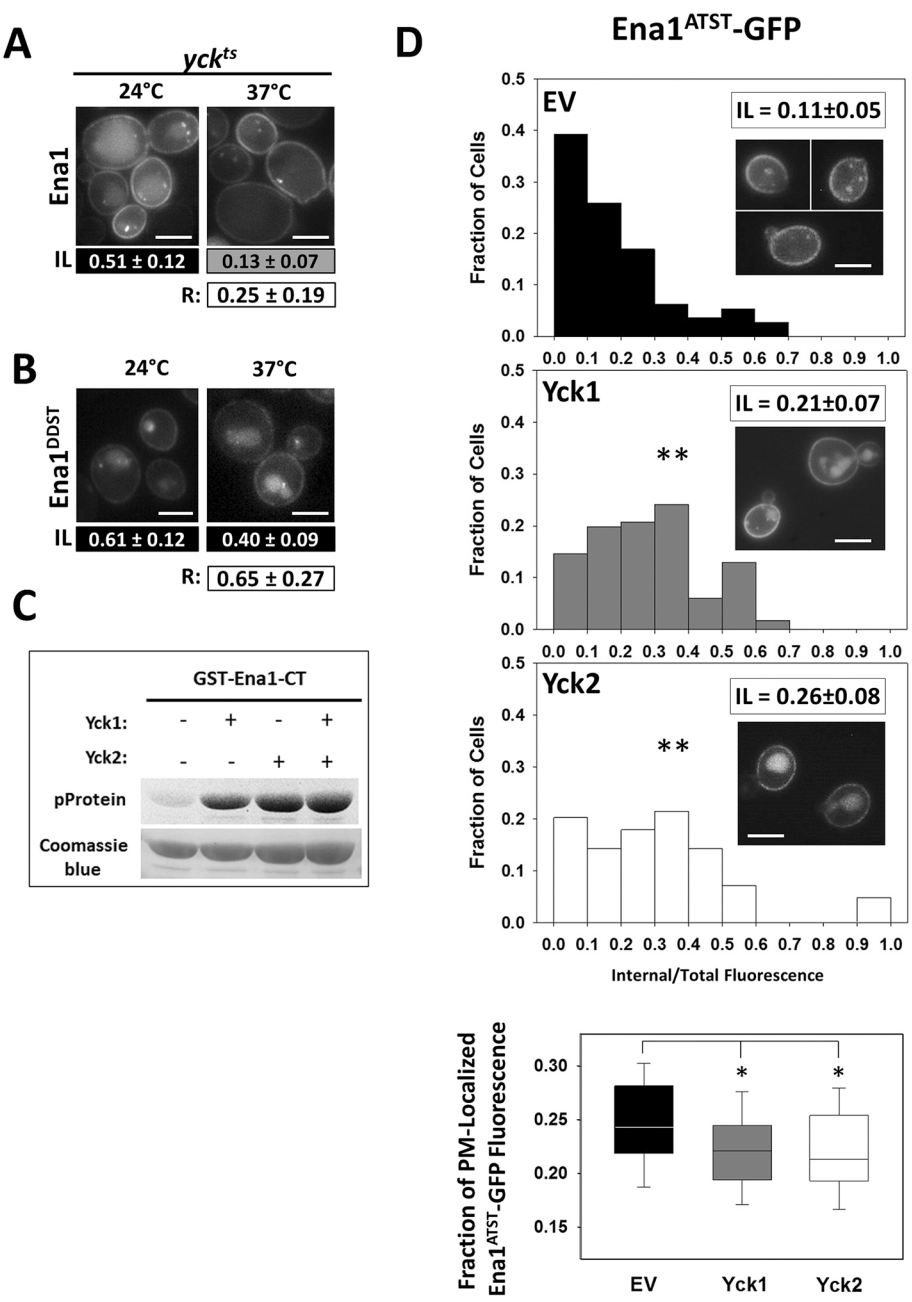

Fig. 7. Ena1 internalization depends on the yeast casein kinases. Intracellular localization of Ena1–GFP (A) and Ena1^{DDST}–GFP (B) was analyzed in *yck^{ts}* cells at permissive (24°C) and restrictive (37°C) temperatures. IL indexes were estimated and analyzed as described in Fig. 1. Representative images are included. Scale bars: 5 µm. 'R' values in white boxes represent the ratio between the corresponding ILs for the monitored Ena1 protein at 37°C to at 24°C (P<0.05). (C) *In vitro* phosphorylation assays were performed by incubating GST–Ena1–CT protein with or without yeast purified Yck1/2 plus ATP. Phosphorylated Ena1–CT and total protein loading is shown (see Materials and Methods for details). (D) Yeast cells expressing the Ena1^{S1076A}–GFP (Ena1^{ATST}) mutant were transformed with empty vector (EV) or plasmids overexpressing Yck1 or Yck2. Ena1^{ATST} relative PM accumulation and IL indexes values (and histograms) in the presence and absence of Yck overexpression, were estimated and statistically analyzed as in Fig. 1. *P<α_C=0.025 [Wilcoxon's test (Ena1^{ATST} PM-accumulation box plots)]. **P≪α_C=0.025 [Kolmogorov–Smirnov test (Ena1^{ATST}–GFP intracellular distribution histograms)]. Representative images are included. Scale bars: 5 µm.

from yeast lysates is able to phosphorylate the Ena1 C-terminus. Therefore, we propose that Yck-mediated phosphorylation of the S^{1076}TST^{1079} patch is required for Ena1 internalization in addition to its ubiquitylation.

K^{1090} and the ST patch are two independent and spatially arranged elements required for Ena1 internalization

S/T phosphorylation has been shown to be a prerequisite for ubiquitylation during internalization of epsin-independent cargoes such as Ste6 (Kelm et al., 2004). We reasoned that if the ST motif was required for Ena1 ubiquitylation, then Ena1^{AAST} mutant with an Ub fused in-frame should bypass this requirement and undergo normal internalization. However, the resulting Ena1^{AAST}–Ub construction exhibited a substantial defect in uptake as compared to WT (Fig. 8A). A complementary experiment showed that Ena1$^{DDST, K1090R}$ was also not internalized efficiently (Fig. 8A).

Although we cannot completely rule out the possibility that the ST patch is required for ubiquitylation and for a Ub-independent activity, taken together, these results strongly suggest that the ST motif and the K^{1090} residue are independently required for epsin-mediated Ena1 internalization. It should be noted that these experiments do not rule out the possibility that phosphorylation of other determinants different from the S^{1076}TST^{1079} play a role in promoting ubiquitylation of Ena1. An important corollary conclusion is that ubiquitylation would be necessary but not sufficient for Ena1 internalization.

To further define characteristics and requirements of this emerging 'STK' epsin-specific combined motif, we investigated whether the spacing between its constitutive elements impacts its function. Therefore, we modified the residue-distance between the transmembrane domain (TM) and the ST patch, as well as the residue separation between the ST patch and K^{1090} by deleting or

Journal of Cell Science (2020) 133, jcs245415. doi:10.1242/jcs.245415

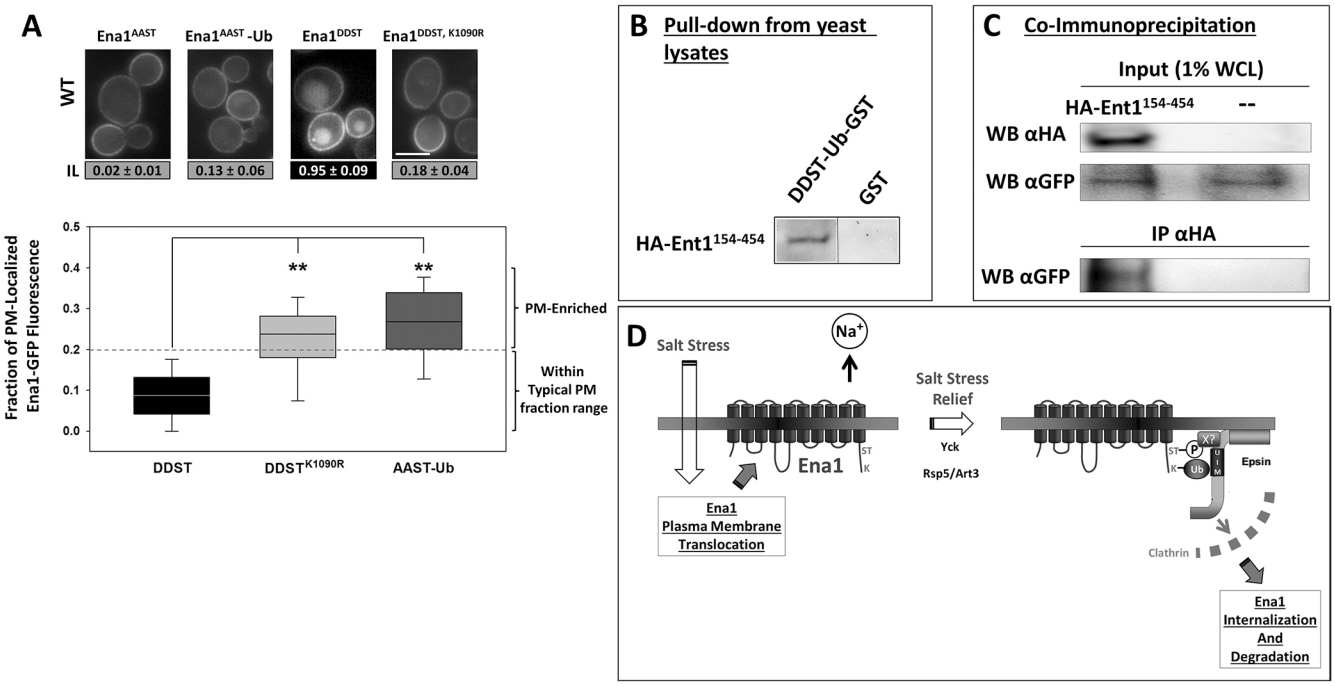

Fig. 8. Characterization of the Ena1 STK epsin-recognition motif. The Ena1–GFP mutants indicated in A were expressed in yeast cells and IL indexes and relative PM accumulation values were estimated as in Fig. 1. Representative images are included. Scale bar: 5 µm. Differences between the Ena1^{DDST} variant and other indicated mutants were statistically analyzed as described in the Materials and Methods and in Fig. 1 using an α_C=0.01. (B) Pulldown from yeast lysates. GSH-beads bearing immobilized GST or DDST–Ub–GST were incubated with lysates from cells expressing HA–Ent1$^{149-454}$ as indicated in the Materials and Methods. The presence of bound HA–Ent1$^{149-454}$ on beads was investigated by western blotting with an anti-HA antibody. (C) Co-immunoprecipitation. These experiments were performed as described in the Materials and Methods. Western blotting (WB) with the indicated antibodies of an input sample (1% of whole-cell lysate used for incubation with beads) show the presence (or absence) of HA–Ent1$^{149-454}$ and Ena1–GFP. Following immunoprecipitation with an anti-HA antibody, the presence of bound Ena1–GFP to the beads was investigated using an anti-GFP antibody (see text for details). (D) Cartoon depicting the proposed mechanism that assures specific recognition of the ubiquitylated cargo Ena1 by the Ub-binding adaptor epsin (see text for details).

duplicating 5-residue long segments of the Ena1 C-terminal sequence. We adopted this approach instead of using artificial spacers to minimize the possibility of introducing changes in flexibility or hydrophobicity that could independently affect Ena1 behavior. However, we cannot completely rule out the possibility that besides spacing, our results may also reflect sequence-specific effects. In fact, our data indicate that eliminating residues between the TM and the ST patch led to ER retention, further supporting the idea that the integrity of the 1050–1070 region is crucial for Ena1 proper folding. In contrast, duplication of the 1066–1070 sequence did not affect the ability of Ena1 to exit the ER and to be internalized (Fig. S6A). When the ST–K residue distance was shortened from 10 to 5 (Δ1083–1087) there were deficiencies in Ena1 uptake, whereas duplication of a 5-residue sequence (1083–1087) did not affect internalization (Fig. S6A). These results suggest that a TM–ST spacing of ≥29 and ST-K of ≥10 sustains proper function of the STK sequence as a combined epsin-specific endocytic motif.

Interestingly, known epsin mammalian cargoes such as VEGFR2, selta-like 1 and ENaC bear C-terminal cytoplasmic sequences with similar composition (rich in serine, threonine or acidic residues) at the appropriate distance from a lysine residue, constituting potentially analogous STK motifs to the one identified in Ena1 (Fig. S6B). In fact, the 'ST'-like motifs from these mammalian proteins were able to functionally replace Ena1 ST patch sustaining epsin-dependent Ena1 internalization (Fig. S6B).

Finally, and to evaluate whether epsin was able to associate with a transporter mutant emulating the double post-translationally modified STK Ena1 motif, we performed pull-down and co-immunoprecipitation (co-IP) experiments.

Epsin pull-down experiments from yeast whole-cell lysates

Glutathione beads bearing immobilized GST or GST–Ub–Ena1$^{S1076D,\ S1077D}$CT as described above and incubated with whole-cell lysates (WCL) from cells expressing HA–Ent1$^{149-454}$ (this truncation was preferred to the more aggregation-prone, ENTH-domain containing, full-length Ent1; see Materials and Methods). After incubation and washes, the beads were boiled in sample buffer, resolved by SDS-PAGE and the presence of bound HA–Ent1$^{149-454}$ investigated by western blotting with anti-HA antibodies. Results shown in Fig. 8B indicate that recombinant 'constitutively phosphorylated/ubiquitylated' cytoplasmic C-terminal tail of Ena1 was able to interact with *in vivo*-produced epsin protein from cell lysates.

Co-immunoprecipitation

Although co-IP of intrinsically low affinity sorting machinery–cargo complexes is challenging (and further aggravated by the presence of ten transmembrane domains in Ena1) we were able to co-immunoprecipitate full-length Ena1$^{S1076D,\ S1077D}$–Ub–GFP with HA-tagged Ent1$^{149-454}$ using an anti-HA antibody (a representative experiment is shown in Fig. 8C). This result indicated that epsin is capable of *in vivo* recognition of constructions that emulate constitutively phosphorylated/ubiquitylated STK from Ena1.

DISCUSSION

Epsin is an endocytic protein essential for cell viability in yeast and required for embryo development in metazoans (Sen et al., 2012). The function of this protein family as endocytic adaptors is necessary for activation of the Notch signaling pathway (Tian et al.,

2004; Wang and Struhl, 2004, 2005) and for the temporal-spatial coordination of endocytosis and RhoGTPase signaling (Aguilar et al., 2006; Coon et al., 2010; Mukherjee et al., 2009). Epsin endocytic function is required for VEGFR2 (Pasula et al., 2012), VEGFR3 (Liu et al., 2014) and ENaC internalization (Staruschenko et al., 2005; Wang et al., 2006) and (although not essential) is known to contribute to the uptake and regulation of EGFR, insulin receptor, mu opioid receptors, dopamine transporter, protease activated receptor 1, Ste2 and others (Bertelsen et al., 2011; Chen et al., 2011; Dores et al., 2010; Hawryluk et al., 2006; Henry et al., 2012; Kazazic et al., 2009; Shih et al., 2002; Sigismund et al., 2005; Sorkina et al., 2006; Sugiyama et al., 2005).

However, how epsin (or any other Ub-binding endocytic adaptors) recognize their specific cargoes among multiple ubiquitylated proteins is unknown. Here, we speculate that there is a coincidence detection mechanism that assures specific recognition of ubiquitylated cargo by yeast epsins. We also suggest that other adaptors, such as the Eps15-homolog Ede1, would require post-translational modification of other determinants (in addition to ubiquitylation) for recognition of their corresponding specific cargoes.

In fact, this study unveils several important aspects of yeast epsin-mediated internalization of cargo. We have established the Na^+ pump Ena1 as the first epsin-specific cargo identified in *S. cerevisiae* and showed that epsins sustain fast internalization of Ena1–GFP upon salt-stress relief. Specific residues within the Ena1 C-terminus ($S^{1076}TST^{1079}$ and K^{1090}) critical for its epsin-mediated internalization were also mapped. Furthermore, our data suggest that the K^{1090} residue is a target for Art3/Rsp5-mediated ubiquitylation, while the ST patch is a target for yeast casein kinase (Yck1/2)-mediated phosphorylation. Our results also support the idea that the two regulatory determinants – Ena1 S^{1076}-T^{1079} and K^{1090} – are independently required for epsin-mediated Ena1 internalization. Therefore, and very importantly, our data also suggest that Ub is not sufficient for Ena1 uptake and suggest the existence of a coincidence detection mechanism for recognition of ubiquitylated cargoes by epsin.

Our results indicate that internalization of Ena1 by epsins does not rely on direct recognition of sequence-encoded sorting signals [such as Y- or L-motifs (Traub and Bonifacino, 2013)], on a double post-translational modification (ubiquitylation and phosphorylation) of specific cargo regions.

On the one hand, Ena1 internalization was dependent on the presence of the arrestin-related adaptor Art3 linking the yeast ubiquitin ligase Rsp5 to this process. This is in agreement with the well-known role of Rsp5 in endocytosis (Rotin et al., 2000). Nevertheless, it is possible that other Ub-ligases might be involved. Although Art9 has been shown to be important for the regulation of Ena1 (Marqués et al., 2015), our data indicates that is not crucial for internalization of the transporter. We speculate that Art9 is involved in the ubiquitylation of K residues relevant to other steps of intracellular traffic while Ena1 K^{1090}-Ub is required for removal from the plasma membrane. On the other hand, our results show that the Ena1 $S^{1076}TST^{1079}$ patch can be indeed phosphorylated *in vivo* and strongly suggest that yeast casein kinases are involved in the transporter uptake. Although we cannot completely rule out involvement of other S/T kinases in Ena1 internalization, our findings are in agreement with the well-known role of Yck proteins in endocytosis (Feng and Davis, 2000; Hicke et al., 1998; Marchal et al., 2002, 2000; Panek et al., 1997).

It has been clearly shown that Yck activity is a pre-requisite for ubiquitylation of the epsin-independent cargoes Ste2 and Ste3 (Ballon et al., 2006; Feng and Davis, 2000; Horák, 2003; Panek et al., 1997). Along the same lines, it has been reported that, following Yck-mediated phosphorylation, several specific ART-family proteins recruit Rsp5, resulting in the ubiquitylation of these cargoes (Alvaro et al., 2016, 2014; Prosser et al., 2015). In contrast, our data indicated that K^{1090} and the ST patch are independently needed for cargo uptake. Nevertheless, it is possible that phosphorylation of other determinants in Ena1 cytoplasmatic domains could support Ena1 ubiquitylation. Therefore, it is tempting to speculate that independence between phosphorylation of this specific ST patch and ubiquitylation in Ena1 is a hallmark of epsin-specific internalization.

Our results also suggest the existence of an epsin-recognized combined STK motif with specific required spacing between its components and from the last transmembrane domain. We speculate that such requirements may reflect steric/spatial constraints for binding the transmembrane STK-bearing cargo by the membrane-bound epsins.

Searching the *S. cerevisiae* database (http://www.yeastgenome.org/), we found several transmembrane proteins displaying putative STK-like sequences with similar spacing and position to that in Ena1 (including the whole Ena protein family). However, the functionality of putative STK motifs for epsin-mediated internalization must be experimentally tested (and it will be the focus of future investigations) as unknown context factors and additional determinants might also play an important role in the control of PM cargo levels.

Indeed, the complexity of the trafficking information packed in the cytosolic (and possibly transmembrane) portions of membrane proteins should not be underestimated. Important work done in the Chen lab clearly indicates that, in mammalian epsins, specificity determinants for the recognition of the receptor tyrosine kinase VEGFR2 are embedded within the UIM sequence environment (Dong et al., 2017, 2015; Rahman et al., 2016). Furthermore, it should be kept in mind that multi-spanning proteins like Ena1 usually contain additional/critical determinants in their intracellular loops; these regions may play a role in the recruitment of post-translational modifying enzymes (e.g. kinases, ubiquitin ligases/ARTs or proteins that may assist in cargo recognition). A binding site for the fly Ub-ligase *Mind bomb* has been found within the cytosolic domain of the epsin cargo protein Delta (Palardy and Chitnis, 2015); very interestingly, this region is flanked by STK-like elements. Furthermore, the simple transplantation of the Ena1 STK motif was not enough to convert Ste3 into an epsin-specific cargo but rendered a plasma membrane-localized hybrid protein. A similar result was observed upon replacement of Ena1 C-terminus for the analogous Ste3 sequence (Fig. S4D). These observations further suggest a complex organization of partially overlapping motifs required for cargo internalization.

Based on our results, we speculate about the specific regulation of the plasma membrane levels of the Na^+ pump Ena1, and propose the following working model (Fig. 8D). Upon salt stress, Ena1 is expressed and translocated to the cell cortex to contribute to the efflux of Na^+ (Yenush, 2016) (Fig. 8D). When salt levels decrease, Ena1 is post-translationally modified by (1) ubiquitylation at K^{1090} (by an Art3–Rsp5 complex) and (2) phosphorylation at the $S^{1076}TSTT^{1080}$ patch (by casein kinases) (Fig. 8D). The double modified C-terminus of Ena1 then becomes competent for specific recognition of yeast epsins and recruitment to nascent endocytic sites by these Ub-binding adaptors. Epsins, in turn, contribute to the binding of accessory factors and the clathrin coat (Sen et al., 2012), which eventually leads to the pinching-off of endocytic vesicles, thereby removing Ena1 from the plasma membrane (Fig. 8D).

Journal of Cell Science (2020) 133, jcs245415. doi:10.1242/jcs.245415

We believe that this model, supporting findings and reagents will be the basis of future investigations that will further our understanding of endocytic function of epsin in yeast. Importantly, one could speculate that alternative coincidence detection mechanisms confer recognition specificity by other ubiquitylated-cargo/ubiquitin-binding adaptor combinations (e.g. involving Ede1). Finally, since mammalian STK motifs sustain Ena1 internalization in yeast, we also speculate that this strategy might be conserved across evolution. Nevertheless, these emerging hypotheses will need to be tested taking into account the complexity (see above) and potential redundancy of endocytic signals and endocytic adaptors.

MATERIALS AND METHODS

Reagents and DNA constructs

Materials were purchased from Thermo Fisher Scientific (Fairlawn, NJ) or Sigma (St Louis, MO) unless stated otherwise. Plasmids and strains used in this study are listed in Tables S2 and S3. DNA constructs were prepared using standard techniques. Site directed mutagenesis was done using a QuikChange® Lightning site directed mutagenesis kit (Agilent Technologies, Inc., Santa Clara, CA).

Yeast culture conditions and transformation procedures

Yeast SEY6210-derived (MATα *leu2-3,112 ura3-52 his3-Δ200 trp1-Δ901 suc2-Δ9 lys2-801; GAL*) and other strains were grown overnight at 30°C (or room temperature for temperature-sensitive strains) with shaking at 250 rpm in standard yeast extract–peptone–dextrose (YPD) or synthetic selective (amino acid dropout) medium supplemented with dextrose and lacking appropriate amino acids for plasmid maintenance. Yeast were transformed by the Li-acetate method following standard techniques.

Microscopy

Images were acquired using a Zeiss Axiovert 200M microscope equipped with a Zeiss Axiocam MRm monochrome digital camera and Carl Zeiss Axiovision image acquisition software (version 4.4). For imaging *MET25* promoter-driven Ena1–GFP-derived constructs, cells were grown overnight in selective medium in the presence of 2 mM methionine. The cultures were diluted, washed with sterile H_2O, and Ena1 expression was induced by growing the cells in selective medium without methionine for 5 h. A cell culture volume containing the equivalent of 2–5 units of optical density at 600 nm (OD_{600nm}) of cells expressing fluorescently tagged proteins were pelleted and resuspended in 50–100 µl selective medium, and 10 µl of cell suspension was spotted on a pre-cleaned slide, covered with a 22×22 mm coverslip and imaged with appropriate filters as ∼0.3 µm-spaced *Z*-stacks.

FM4-64 staining

To visualize the endocytic pathway and vacuolar membrane, staining using FM4-64 was performed according to Baggett et al. (2003). Briefly, cells were grown overnight to 0.3–0.8 OD_{600}/ml in selective medium. 1 ml of cells were pelleted and chilled on ice, followed by the addition of cold FM4-64 (1:40 dilution from a stock of 1 mg/ml in DMSO) in a final volume of 50 µl of selective medium. The cells were incubated for 15–20 min on ice and subsequently imaged (*t*=0 min). Cells were supplemented with 900 µl of fresh pre-warmed selective medium and allowed to incubate at 30°C for 30 min. At this time point, cells were quickly chilled on ice prior to imaging at 100× using GFP and Rhodamine filters.

Quantitative analysis of Ena1–GFP localization

To quantify the localization of fluorescently tagged Ena1, we used an approach based on the analysis of fluorescence signal distribution within cells in randomly acquired images. First, we manually outlined each cell and measured the total GFP fluorescence intensity (T) using ImageJ software. T represents the sum of fluorescence contributions associated with the internal compartments (I), plasma membrane-localized signal (P) and cytosolic background (C). The fluorescence intensity inside of the cell (I_C=I+C) was measured by outlining the cell of interest excluding the peripheral region, while the P component value was estimated subtracting I_C from T. The average contribution of cytosolic fluorescence was quantified by measuring and averaging the fluorescence intensity of three rectangular regions within the cytosol of each analyzed cell. This value multiplied by the cell area yielded an integrated cytosolic background intensity (C). Internal fluorescence intensity was calculated as $I=I_C-C$. The I component arises from endocytic uptake of Ena1–GFP as shown by >95% colocalization with the hydrophobic dye FM4-64 (Fig. S2). All measurements were performed on a single plane with the best focus of cell periphery. This analysis was performed on at least 30 cells and each experiment was performed at three 3 times.

The results were processed and represented in two complementary ways. First, histograms (fraction of cells vs I/T values) provided a measurement population distribution. In addition to direct histogram comparisons, an 'intracellular localization' (IL) index was defined as the cumulative fraction of cells with intracellular fluorescence greater than 50% of the total fluorescence (i.e. the fraction of cells present at the right-hand side of a line positioned at I/T=0.5 over at least three histograms). This value integration procedure yielded a normally distributed, very convenient descriptor of population skewness with respect to Ena1–GFP localization. The higher the IL, the higher the proportion of cells with cargo enrichment in intracellular compartments. Second, we analysed *P/T* median values to provide a measure of Ena1–GFP plasma membrane accumulation in cells. Since $P=T-I_C$ (see above), the calculation of this quantity does not require estimation of cytosolic background, thereby decreasing error propagation. Although showing typical cell-to-cell biological variation (and following a non-normal distribution), P/T values were found to be fairly independent of Ena1–GFP levels of expression (Fig. S3C). Nevertheless, highly overexpressing cells were excluded from all analyses. A P/T median value ≤0.2 (Fig. S3C) was considered within the limits for typical (normal) Ena1-GFP PM fraction range.

It should be noted that populations with similar ILs can show substantially different P/T median values.

Salt stress relief assay

WT and *ent1Δent2Δ* cells expressing Ena1–GFP were grown overnight in selective medium supplemented with 0.2 mM methionine to maintain low levels of Ena1 expression (controlled by *MET25* methionine-repressible promoter). Cells were grown to early log phase, washed and transferred to medium lacking methionine for 2 h, thereby inducing high Ena1 expression for a short time. Next, 0.5 M NaCl was added to the cells to simulate salt stress and simultaneously supplemented with 2 mM methionine to suppress the *MET25* promoter (stopping Ena1 production), and cells were incubated under these conditions for 3 h. This was done to ensure that the Ena1–GFP produced by the cells would be recruited and maintained at the cell membrane to pump out excess sodium. The cells were imaged (time 0), and then washed to remove NaCl excess ('salt stress relief' – under these conditions we expected Ena1 to be internalized) and resuspended in medium containing 2 mM methionine. Cells were imaged over time and the amount of peripherally localized Ena1 was quantified.

Flow cytometry

WT or *ent1Δent2Δ* cells transformed with Ena1–GFP plasmid were cultured in synthetic complete medium lacking methionine at 30°C overnight. The cells were diluted to 0.2 OD_{600nm}/ml with fresh medium and grown for 2 h. Cells were supplemented with methionine to a 2 mM final concentration, and a sample was taken immediately after ('0 h'), and another after 5 h incubation at 30°C ('5 h'). After staining with propidium iodide (BD Biosciences) for 10 min, 5×10^4 cells were analyzed using a FC500 flow cytometer (Beckman-Coulter) with FL1 and FL3 detectors. The results were processed using FlowJo v7.6 software.

Cell lysate preparation

Cells were grown in selective medium and spheroplasted following standard techniques (Katzmann and Wendland, 2005). Briefly, cells at ∼50 OD_{600} were harvested and incubated for 10 min at room temperature in softening solution [0.1 M Tris-HCl pH 9.4, 10 mM DTT and 5 mM N-ethylmaleimide (NEM)]. Cells were then resuspended in spheroplasting solution composed of YPD medium containing 1 M sorbitol, 1 unit of zymolyase per OD_{600}, protease inhibitor cocktail (Pierce) and 0.1 mM 4-(2-aminoethyl)benzenesulfonyl fluoride (AEBSF) for 30 min at 30°C. Spheroplasts were washed once with

Journal of Cell Science (2020) 133, jcs245415. doi:10.1242/jcs.245415

PBS containing 1 M sorbitol, pelleted by centrifugation at 300 ***g*** for 5 min and dounce-homogenized with in HEPES/KOAc lysis buffer (0.2 M sorbitol, 50 mM KOAc, 2 mM EDTA, 20 mM HEPES pH 6.8, 0.2% Triton X-100, 50 mM NEM and protease inhibitor cocktail).

Western blotting

For Ena1–GFP detection by western blotting, cells were induced to express Ena1–GFP (WT or mutant) by maintaining them in medium without methionine for 5 h. The equivalent to 10 OD_{600} of cells were collected and resuspended in 200 µl of 0.2 M NaOH for 15 min at room temperature. Cells were spun down at 1000 ***g*** for 2 min and resuspended in 50 µl of 2× Laemmli buffer with 8% SDS (100 mM Tris-HCl pH 6.8, 8% SDS, 40% glycerol, 2% mercaptoethanol, 0.005% Bromophenol Blue) and incubated at 55°C for 15 min. The equivalent to 50 µl of 0.15-0.25 mm acid washed beads were added to the sample and vortexed for 1 min at room temperature. The samples were chilled on ice for 2 min and spun down at 300 ***g*** for 5 min. The supernatants were collected and resolved on 8% SDS-PAGE gels, transferred onto nitrocellulose followed by immunoblotting using an anti-GFP antibody (Thermo Fisher Scientific, A-11122) at a 1:1000 dilution. The loading control, VDAC1 (porin) was detected by using a specific mouse monoclonal antibody (clone 16G9E6BC4, Thermo Fisher Scientific) at 1:1000 dilution. Blots were developed using the enhanced chemiluminescence detection system.

Crude membrane preparation

Cells expressing Ena1–GFP were grown overnight in the presence of 0.2 mM methionine. Cells were diluted in medium without methionine to a final 0.5 OD_{600}/ml and to induce Ena1–GFP expression for 5 h. Cells at 200 OD_{600} were collected by centrifugation at 1000 ***g*** for 5 min, resuspended in ice-cold water and aliquoted to give 10 OD_{600}/tube. The cells were then pelleted down at 2000 ***g*** for 2 min, and 0.15–0.25 mm acid-washed glass beads (equivalent to a 100 µl volume) and 1 ml of ice-cold lysis buffer [30 mM Tris-HCl pH 7.5, 5 mM EDTA, 25 mM DTT, 250 mM NaF, 2× protease inhibitors and 2× phosphatase inhibitor cocktails (Pierce)] were added to each tube. The cells were broken by vortexing for 3 min, then chilled on ice for 2 min, repeating the cycle twice. The crude membranes were collected by pelleting the lysates at 300 ***g*** for 5 min, the supernatants were pooled and centrifuged at 20,000 ***g*** 30 min at 4°C. The pellet was resuspended in 1 ml of lysis buffer containing 0.1% SDS.

Mass spectrometry

Protein extraction and phosphopeptide enrichment

GFP-tagged Ena1 was purified by incubating extracted crude membranes with GFP-Trap agarose beads (ChromoTek, NY) for 1 h at 4°C. The GFP-Trap beads were washed with RIPA buffer (50 mM Tris-HCl pH 7.5, 150 mM NaCl, 1% NP-40, 0.5 mM EDTA, 0.1% SDS, 0.5% sodium deoxycholate, and 50 mM NaF) three times, and enriched Ena1–GFP proteins were denatured in 8 M urea and reduced with 5 mM dithiothreitol for 30 min at 37°C. The proteins were further alkylated in 15 mM iodoacetamide for 1 h in the dark at room temperature and then digested with proteomics grade trypsin at a 1:100 (w/w) ratio overnight at 37°C. The digested peptides were desalted by SDB-XC reverse phase-Stage Tips (Rappsilber et al., 2007). Phosphopeptides from Ena1–GFP were enriched by polyMAC (Iliuk et al., 2010). The eluted phosphopeptides were dried in a SpeedVac and stored at −20°C.

LC-MS/MS analysis and data analysis

The phosphopeptides were dissolved in 4 µl of 0.1% formic acid and injected into an Easy-nLC 1000 (Thermo Fisher Scientific). The mobile phase buffer consisted of 0.1% formic acid in ultra-pure water (buffer A) with an eluting buffer of 0.1% formic acid in 80% ACN (buffer B) run over a linear 90 min gradient with a flow rate of 250 nl/min. The Easy-nLC 1000 was coupled online with a Velos LTQ-Orbitrap mass spectrometer (Thermo Fisher Scientific). The mass spectrometer was operated in the data-dependent mode in which a full-scan MS (from *m*/*z* 300–1500 with the resolution of 60,000 at *m*/*z* 400) was followed by top 15 MS/MS scans of the most abundant ions. The raw files were searched directly against the *S. cerevisiae* database (UniprotKB) with no redundant entries using both the SEQUEST HT and BYONIC algorithm on Proteome Discoverer™ version 2.0 (Thermo Fisher Scientific). Peptide precursor mass tolerance was set at 10 ppm, and MS/MS tolerance was set at 0.6 Da. Search criteria included a static carbamidomethylation of cysteine residues (+57.0214 Da) and variable modifications of (1) oxidation (+15.9949 Da) on methionine residues, (2) Gln to pyro-Glu (−17.027 Da) at the N-terminus of peptides, (3) acetylation (+42.011 Da) at N-terminus of proteins, and (4) phosphorylation (+79.996 Da) on serine, threonine or tyrosine residues were searched. Searching was performed with full tryptic digestion and allowed a maximum of two missed cleavages on the peptides analyzed from the sequence database. Relaxed and strict false discovery rates (FDR) were set for 0.05 and 0.01, respectively.

Recombinant protein purification

Bacterially produced recombinant proteins were purified based on the procedure described in Aguilar et al. (2003). Rosetta cells (Novagen) were transformed with GST- or His_6-tagged constructs (listed in Table S1) and protein production was induced by incubation with 0.2 mM (final concentration) isopropyl-β-D-thiogalactopyranoside (IPTG) for 5 h at 30°C. The cells were harvested and resuspended in PBS containing 0.1% Tween (PBST) plus 5% glycerol, protease inhibitor cocktail and 0.1 mM AEBSF. Cell lysis was induced by incubating the cell suspension with 1 mg/ml lysozyme (4°C, 15 min) followed by sonication. Clarified lysates were incubated either with Ni-NTA beads in the presence of 5 mM imidazole (for purification of His_6-tagged proteins) or with glutathione-coupled beads (for purification of GST-tagged proteins), for 2 h at 4°C. The beads were washed four times with PBST with imidazole (in increasing concentrations of 5 mM, 10 mM, 15 mM and 20 mM) for His_6-tagged proteins, and four times with PBST alone for GST-tagged proteins. Elution was performed with either 500 mM imidazole (His_6-tagged proteins) or 50 mM glutathione (GST-tagged proteins). The supernatants containing the purified tagged proteins were collected, and the imidazole from His_6-tagged and glutathione from GST tagged protein fractions were removed using Zeba™ spin desalting columns (Thermo Scientific, Waltham, MA).

In vitro kinase assay

C-terminal His_6-tagged Yck1/2 proteins were expressed in yeast and purified from whole-cell lysates (equivalent to ∼100 OD_{600} of cells) using Ni^{2+}-NTA beads and eluted with 500 µl of 500 mM imidazole and desalted into 500 µl of 2× kinase buffer (100 mM Tris-HCl pH 7.5, 20 mM $MgCl_2$, 2 mM DTT). Purified Yck1/2 proteins were incubated with GST–$Ena1^{K1090R}$CT–Ub immobilized on 50 µl of glutathione beads at 30°C for 45 min in 1× kinase buffer with 5 mM ATP. The beads were then washed three times with 1× kinase buffer and boiled with 25 µl of 2× protein sample buffer. Samples were resolved with SDS-PAGE and phosphorylated proteins were detected using the Pro-Q® Diamond phosphoprotein gel stain kit (ThermoScientific, Waltham, MA) following the manufacturer's instructions.

Pulldown assay with cell lysate and recombinant proteins

Overexpression of HA–$Ent1^{149\text{-}454}$ under the regulation of a *MET25* promoter was induced by growing the cells overnight in selective medium in the absence of methionine. For these and for co-immunoprecipitation experiments, the Ent1 truncation indicated above was preferred to the more aggregation-prone, ENTH-domain containing, full-length Ent1. Cell lysates were prepared as described above. The samples were centrifuged at 5000 ***g*** for 5 min, and clarified lysates were incubated with GST or GST fusion proteins immobilized on glutathione-coupled beads for 2 h at room temperature. The beads were washed five times with PBST, resuspended in Laemmli's protein sample buffer, followed by SDS-PAGE resolution and immunoblotting. A mouse monoclonal anti-HA antibody was used (Cat# MMS-101R, Covance, Princeton, NJ) at 1:2500 dilution.

Co-immunoprecipitation assay

Yeast cells expressing *MET25* promoter-driven Ena1–GFP transformed with empty vector or a plasmid encoding for HA-tagged $Ent1^{149\text{-}454}$ (under the endogenous promoter), were grown overnight in selective medium in the

absence of methionine. Cells were lysed by spheroplasting and dounce homogenization as described above and subjected to cross-linking using 2 mM DSP [Dithiobis (succinimidyl propionate)] for 30 min at room temperature with constant rotation. The crosslinking reaction was quenched by incubating with 50 mM Tris-HCl pH 7.5 for 15 min. For protein extraction, mild alkali treatment was used (Kushnirov, 2000). NaOH was added to the mix to a final concentration of 0.2 M and incubated for 5 min at RT. Samples were centrifuged at 5000 ***g*** for 5 min and the supernatant was discarded. The pellet was resuspended in extraction buffer (0.06 M Tris-HCl pH 7.5, 1% SDS, 5% glycerol, 2% β-mercaptoethanol, supplemented with NEM, protease and phosphatase inhibitors) and boiled for 3 min. Following centrifugation at 5000 ***g*** for 5 min, the clarified supernatant was diluted at least 20 times in 1 M Tris-HCl pH 7.5. Anti-HA coupled beads (EZview red anti-HA affinity gel, Sigma) were used to immunoprecipitate HA-tagged proteins (at 4°C for 2 h). Following three washes, the beads were boiled in Laemmli buffer for 5 min. Samples were resolved by SDS-PAGE and immunoblotted. A rabbit monoclonal anti-GFP antibody (Cat# G10362, Invitrogen, Carlsbad, CA) at 1:10 dilution was used to detect GFP-tagged proteins from the immunoprecipitates. HA tagged proteins were detected using a mouse monoclonal α-HA antibody (Cat# MMS-101R, Covance, Princeton, NJ) at 1:2500 dilution.

Ena1–GFP Ub-affinity capture

Cells were induced to express Ena1–GFP (WT or mutant) by maintaining them in medium without methionine for 5 h. Cells at ∼100 OD_{600} were spheroplasted as described in the previous section (see Cell lysate preparation). Total ubiquitylated proteins were affinity-captured using Ubiquitin Affinity beads (UBA01; which uses a proprietary formulation of ubiquitin-binding domain proteins able to detect difficult targets such as mono-ubiquitylated products) included in the Signal-Seeker™ ubiquitylation detection kit (Cytoskeleton Cat. #BK161) following the manufacturer's instructions. The Ena1-GFP from samples and 5% input lysates were resolved in 8% SDS-PAGE gels, transferred onto nitrocellulose followed by immuno-blotting using an anti-GFP antibody (Thermo Fisher A-11122) at a 1:1000 dilution.

Statistical analysis

The analysis was performed as described below and in Taylor (1997). When appropriate, the magnitude of errors associated with values derived from algebraic operations using experimentally measured quantities were calculated following standard rules of error propagation. Statistical significance of differences between fluorescence distribution histograms were analyzed using the Kolmogorov–Smirnov test. The Student's *t*-test was used to evaluate differences among normally distributed ILs, while the Wilcoxon's test was used to evaluate the significance between non-normal P/T of value samples. Bonferroni's correction for multiple comparisons was performed whenever applicable [α_C=p/*n*; *n* being the number of comparisons].

Acknowledgements

We thank Drs Chris Staiger, Donald Ready, Henry Chang and Tony Hazbun (Purdue University) for stimulating discussions and/or critical reading of the manuscript. We thank Dr Jeremy Thorner (UC Berkeley) for strains and for graciously allowing the use of his lab space and equipment. We also thank Drs Lucy Robinson (Louisiana State University), Ingrid Wadskog (Göteborg University) and Martha Cyert (Stanford) for reagents.

Competing interests

The authors declare no competing or financial interests.

Author contributions

Conceptualization: R.C.A.; Formal analysis: A.S., W.-C.H., R.C.A.; Investigation: A.S., W.-C.H., C.B.H., C.-C.H., M.P., W.A.T., R.C.A.; Resources: R.C.A.; Writing - original draft: A.S., W.-C.H., R.C.A.; Writing - review & editing: R.C.A.; Visualization: R.C.A.; Supervision: W.A.T., R.C.A.; Project administration: R.C.A.; Funding acquisition: R.C.A.

Funding

This work was supported by the National Science Foundation under grant no. 1021377 to R.C.A. and by the Center for Science of Information (CSoI), an NSF ST Center, under grant CCF-0939370.

Supplementary information

Supplementary information available online at
https://jcs.biologists.org/lookup/doi/10.1242/jcs.245415.supplemental

References

Aguilar, R. C., Watson, H. A. and Wendland, B. (2003). The yeast Epsin Ent1 is recruited to membranes through multiple independent interactions. *J. Biol. Chem.* **278**, 10737-10743. doi:10.1074/jbc.M211622200

Aguilar, R. C., Longhi, S. A., Shaw, J. D., Yeh, L.-Y., Kim, S., Schon, A., Freire, E., Hsu, A., McCormick, W. K., Watson, H. A. et al. (2006). Epsin N-terminal homology domains perform an essential function regulating Cdc42 through binding Cdc42 GTPase-activating proteins. *Proc. Natl. Acad. Sci. USA* **103**, 4116-4121. doi:10.1073/pnas.0510513103

Alvaro, C. G., O'Donnell, A. F., Prosser, D. C., Augustine, A. A., Goldman, A., Brodsky, J. L., Cyert, M. S., Wendland, B. and Thorner, J. (2014). Specific alpha-arrestins negatively regulate Saccharomyces cerevisiae pheromone response by down-modulating the G-protein-coupled receptor Ste2. *Mol. Cell. Biol.* **34**, 2660-2681. doi:10.1128/MCB.00230-14

Alvaro, C. G., Aindow, A. and Thorner, J. (2016). Differential phosphorylation provides a switch to control how alpha-Arrestin Rod1 down-regulates mating pheromone response in Saccharomyces cerevisiae. *Genetics* **203**, 299-317. doi:10.1534/genetics.115.186122

Artigas, P. and Gadsby, D. C. (2002). Ion channel-like properties of the Na+/K+ Pump. *Ann. N. Y. Acad. Sci.* **976**, 31-40. doi:10.1111/j.1749-6632.2002.tb04711.x

Baggett, J. J., Shaw, J. D., Sciambi, C. J., Watson, H. A. and Wendland, B. (2003). Fluorescent labeling of yeast. *Curr. Protoc. Cell Biol.* **20**, 4.13.1-4.13.28. doi:10.1002/0471143030.cb0413s20

Ballon, D. R., Flanary, P. L., Gladue, D. P., Konopka, J. B., Dohlman, H. G. and Thorner, J. (2006). DEP-domain-mediated regulation of GPCR signaling responses. *Cell* **126**, 1079-1093. doi:10.1016/j.cell.2006.07.030

Becuwe, M., Herrador, A., Haguenauer-Tsapis, R., Vincent, O. and Léon, S. (2012). Ubiquitin-mediated regulation of endocytosis by proteins of the arrestin family. *Biochem. Res. Int.* **2012**, 242764. doi:10.1155/2012/242764

Belgareh-Touze, N., Leon, S., Erpapazoglou, Z., Stawiecka-Mirota, M., Urban-Grimal, D. and Haguenauer-Tsapis, R. (2008). Versatile role of the yeast ubiquitin ligase Rsp5p in intracellular trafficking. *Biochem. Soc. Trans.* **36**, 791-796. doi:10.1042/BST0360791

Bertelsen, V., Sak, M. M., Breen, K., Rødland, M. S., Johannessen, L. E., Traub, L. M., Stang, E. and Madshus, I. H. (2011). A chimeric pre-ubiquitinated EGF receptor is constitutively endocytosed in a clathrin-dependent, but kinase-independent manner. *Traffic* **12**, 507-520. doi:10.1111/j.1600-0854.2011.01162.x

Chen, B., Dores, M. R., Grimsey, N., Canto, I., Barker, B. L. and Trejo, J. (2011). AP-2 and epsin-1 mediate protease-activated receptor-1 internalization via phosphorylation- and ubiquitination-dependent sorting signals. *J. Biol. Chem.* **286**, 40760-40770. doi:10.1074/jbc.M111.299776

Coon, B. G., Burgner, J., Camonis, J. H. and Aguilar, R. C. (2010). The epsin family of endocytic adaptors promotes fibrosarcoma migration and invasion. *J. Biol. Chem.* **285**, 33073-33081. doi:10.1074/jbc.M110.124123

Dong, Y., Wu, H., Rahman, H. N. A., Liu, Y., Pasula, S., Tessneer, K. L., Cai, X., Liu, X., Chang, B., McManus, J. et al. (2015). Motif mimetic of epsin perturbs tumor growth and metastasis. *J. Clin. Invest.* **125**, 4349-4364. doi:10.1172/JCI80349

Dong, Y., Wu, H., Dong, J., Song, K., Rahman, H. A., Towner, R. and Chen, H. (2017). Mimetic peptide of ubiquitin-interacting motif of epsin as a cancer therapeutic-perspective in brain tumor therapy through regulating VEGFR2 signaling. *Vessel Plus* **1**, 3-11. doi:10.20517/2574-1209.2016.01

Dores, M. R., Schnell, J. D., Maldonado-Baez, L., Wendland, B. and Hicke, L. (2010). The function of yeast epsin and Ede1 ubiquitin-binding domains during receptor internalization. *Traffic* **11**, 151-160. doi:10.1111/j.1600-0854.2009.01003.x

Dunn, R. and Hicke, L. (2001). Domains of the Rsp5 ubiquitin-protein ligase required for receptor-mediated and fluid-phase endocytosis. *Mol. Biol. Cell* **12**, 421-435. doi:10.1091/mbc.12.2.421

Feng, Y. and Davis, N. G. (2000). Akr1p and the type I casein kinases act prior to the ubiquitination step of yeast endocytosis: Akr1p is required for kinase localization to the plasma membrane. *Mol. Cell. Biol.* **20**, 5350-5359. doi:10.1128/MCB.20.14.5350-5359.2000

Gadsby, D. C. (2009). Ion channels versus ion pumps: the principal difference, in principle. *Nat. Rev. Mol. Cell Biol.* **10**, 344-352. doi:10.1038/nrm2668

Galan, J. M., Moreau, V., Andre, B., Volland, C. and Haguenauer-Tsapis, R. (1996). Ubiquitination mediated by the Npi1p/Rsp5p ubiquitin-protein ligase is required for endocytosis of the yeast uracil permease. *J. Biol. Chem.* **271**, 10946-10952. doi:10.1074/jbc.271.18.10946

Garciadeblas, B., Rubio, F., Quintero, F. J., Bañuelos, M. A., Haro, R. and Rodríguez-Navarro, A. (1993). Differential expression of two genes encoding isoforms of the ATPase involved in sodium efflux in Saccharomyces cerevisiae. *Mol. Gen. Genet.* **236**, 363-368. doi:10.1007/BF00277134

Girão, H., Catarino, S. and Pereira, P. (2009). Eps15 interacts with ubiquitinated Cx43 and mediates its internalization. *Exp. Cell Res.* **315**, 3587-3597. doi:10.1016/j.yexcr.2009.10.003

Gitan, R. S. and Eide, D. J. (2000). Zinc-regulated ubiquitin conjugation signals endocytosis of the yeast ZRT1 zinc transporter. *Biochem. J.* **346**, 329-336. doi:10.1042/bj3460329

Haro, R., Garciadeblas, B. and Rodríguez-Navarro, A. (1991). A novel P-type ATPase from yeast involved in sodium transport. *FEBS Lett.* **291**, 189-191. doi:10.1016/0014-5793(91)81280-L

Hawryluk, M. J., Keyel, P. A., Mishra, S. K., Watkins, S. C., Heuser, J. E. and Traub, L. M. (2006). Epsin 1 is a polyubiquitin-selective clathrin-associated sorting protein. *Traffic* **7**, 262-281. doi:10.1111/j.1600-0854.2006.00383.x

Helenius, I. T., Dada, L. A. and Sznajder, J. I. (2010). Role of ubiquitination in Na,K-ATPase regulation during lung injury. *Proc. Am. Thorac. Soc.* **7**, 65-70. doi:10.1513/pats.200907-082JS

Henry, A. G., Hislop, J. N., Grove, J., Thorn, K., Marsh, M. and von Zastrow, M. (2012). Regulation of endocytic clathrin dynamics by cargo ubiquitination. *Dev. Cell* **23**, 519-532. doi:10.1016/j.devcel.2012.08.003

Hicke, L. and Riezman, H. (1996). Ubiquitination of a yeast plasma membrane receptor signals its ligand-stimulated endocytosis. *Cell* **84**, 277-287. doi:10.1016/S0092-8674(00)80982-4

Hicke, L., Zanolari, B. and Riezman, H. (1998). Cytoplasmic tail phosphorylation of the alpha-factor receptor is required for its ubiquitination and internalization. *J. Cell Biol.* **141**, 349-358. doi:10.1083/jcb.141.2.349

Horák, J. (2003). The role of ubiquitin in down-regulation and intracellular sorting of membrane proteins: insights from yeast. *Biochim. Biophys. Acta* **1614**, 139-155. doi:10.1016/S0005-2736(03)00195-0

Iliuk, A. B., Martin, V. A., Alicie, B. M., Geahlen, R. L. and Tao, W. A. (2010). In-depth analyses of kinase-dependent tyrosine phosphoproteomes based on metal ion-functionalized soluble nanopolymers. *Mol. Cell. Proteomics* **9**, 2162-2172. doi:10.1074/mcp.M110.000091

Katzmann, D. J. and Wendland, B. (2005). *Ubiquitin and Protein Degradation, Part B*, Vol. 399, 1st edn.: Elsevier Academic Press.

Kazazic, M., Bertelsen, V., Pedersen, K. W., Vuong, T. T., Grandal, M. V., Rødland, M. S., Traub, L. M., Stang, E. and Madshus, I. H. (2009). Epsin 1 is involved in recruitment of ubiquitinated EGF receptors into clathrin-coated pits. *Traffic* **10**, 235-245. doi:10.1111/j.1600-0854.2008.00858.x

Kelm, K. B., Huyer, G., Huang, J. C. and Michaelis, S. (2004). The internalization of yeast Ste6p follows an ordered series of events involving phosphorylation, ubiquitination, recognition and endocytosis. *Traffic* **5**, 165-180. doi:10.1111/j.1600-0854.2004.00168.x

Kushnirov, V. V. (2000). Rapid and reliable protein extraction from yeast. *Yeast* **16**, 857-860. doi:10.1002/1097-0061(20000630)16:9<857::AID-YEA561>3.0.CO;2-B

Lauwers, E., Erpapazoglou, Z., Haguenauer-Tsapis, R. and André, B. (2010). The ubiquitin code of yeast permease trafficking. *Trends Cell Biol.* **20**, 196-204. doi:10.1016/j.tcb.2010.01.004

Lecuona, E., Trejo, H. E. and Sznajder, J. I. (2007). Regulation of Na,K-ATPase during acute lung injury. *J. Bioenerg. Biomembr.* **39**, 391-395. doi:10.1007/s10863-007-9102-1

Lin, A. and Man, H.-Y. (2014). Endocytic adaptor epidermal growth factor receptor substrate 15 (Eps15) is involved in the trafficking of ubiquitinated α-amino-3-hydroxy-5-methyl-4-isoxazolepropionic acid receptors. *J. Biol. Chem.* **289**, 24652-24664. doi:10.1074/jbc.M114.582114

Lin, C. H., MacGurn, J. A., Chu, T., Stefan, C. J. and Emr, S. D. (2008). Arrestin-related ubiquitin-ligase adaptors regulate endocytosis and protein turnover at the cell surface. *Cell* **135**, 714-725. doi:10.1016/j.cell.2008.09.025

Liu, X., Pasula, S., Song, H., Tessneer, K. L., Dong, Y., Hahn, S., Yago, T., Brophy, M. L., Chang, B., Cai, X. et al. (2014). Temporal and spatial regulation of epsin abundance and VEGFR3 signaling are required for lymphatic valve formation and function. *Sci. Signal.* **7**, ra97. doi:10.1126/scisignal.2005413

Logg, K., Warringer, J., Hashemi, S. H., Käll, M. and Blomberg, A. (2008). The sodium pump Ena1p provides mechanistic insight into the salt sensitivity of vacuolar protein sorting mutants. *Biochim. Biophys. Acta* **1783**, 974-984. doi:10.1016/j.bbamcr.2008.02.022

Maldonado-Báez, L., Dores, M. R., Perkins, E. M., Drivas, T. G., Hicke, L. and Wendland, B. (2008). Interaction between epsin/Yap180 adaptors and the scaffolds Ede1/Pan1 is required for endocytosis. *Mol. Biol. Cell* **19**, 2936-2948. doi:10.1091/mbc.e07-10-1019

Marchal, C., Haguenauer-Tsapis, R. and Urban-Grimal, D. (2000). Casein kinase I-dependent phosphorylation within a PEST sequence and ubiquitination at nearby lysines signal endocytosis of yeast uracil permease. *J. Biol. Chem.* **275**, 23608-23614. doi:10.1074/jbc.M001735200

Marchal, C., Dupré, S. and Urban-Grimal, D. (2002). Casein kinase I controls a late step in the endocytic trafficking of yeast uracil permease. *J. Cell Sci.* **115**, 217-226.

Marqués, M. C., Zamarbide-Forés, S., Pedelini, L., Llopis-Torregrosa, V. and Yenush, L. (2015). A functional Rim101 complex is required for proper accumulation of the Ena1 Na+-ATPase protein in response to salt stress in Saccharomyces cerevisiae. *FEMS Yeast Res.* **15**, fov017. doi:10.1093/femsyr/fov017

McNatt, M. W., McKittrick, I., West, M. and Odorizzi, G. (2007). Direct binding to Rsp5 mediates ubiquitin-independent sorting of Sna3 via the multivesicular body pathway. *Mol. Biol. Cell* **18**, 697-706. doi:10.1091/mbc.e06-08-0663

Mukherjee, D., Coon, B. G., Edwards, D. F., Hanna, C. B., Longhi, S. A., McCaffery, J. M., Wendland, B., Retegui, L. A., Bi, E. and Aguilar, R. C. (2009). The yeast endocytic protein Epsin 2 functions in a cell-division signaling pathway. *J. Cell Sci.* **122**, 2453-2463. doi:10.1242/jcs.041137

Mukhopadhyay, D. and Riezman, H. (2007). Proteasome-independent functions of ubiquitin in endocytosis and signaling. *Science* **315**, 201-205. doi:10.1126/science.1127085

Nikko, E. and Pelham, H. R. B. (2009). Arrestin-mediated endocytosis of yeast plasma membrane transporters. *Traffic (Copenhagen, Denmark)* **10**, 1856-1867. doi:10.1111/j.1600-0854.2009.00990.x

Nikko, E., Sullivan, J. A. and Pelham, H. R. B. (2008). Arrestin-like proteins mediate ubiquitination and endocytosis of the yeast metal transporter Smf1. *EMBO Rep.* **9**, 1216-1221. doi:10.1038/embor.2008.199

Oestreich, A. J., Aboian, M., Lee, J., Azmi, I., Payne, J., Issaka, R., Davies, B. A. and Katzmann, D. J. (2007). Characterization of multiple multivesicular body sorting determinants within Sna3: a role for the ubiquitin ligase Rsp5. *Mol. Biol. Cell* **18**, 707-720. doi:10.1091/mbc.e06-08-0680

Overstreet, E., Fitch, E. and Fischer, J. A. (2004). Fat facets and Liquid facets promote Delta endocytosis and Delta signaling in the signaling cells. *Development* **131**, 5355-5366. doi:10.1242/dev.01434

Palardy, G. and Chitnis, A. B. (2015). Identification of the mind Bomb1 Interaction domain in Zebrafish DeltaD. *PLoS ONE* **10**, e0127864. doi:10.1371/journal.pone.0127864

Panek, H. R., Stepp, J. D., Engle, H. M., Marks, K. M., Tan, P. K., Lemmon, S. K. and Robinson, L. C. (1997). Suppressors of YCK-encoded yeast casein kinase 1 deficiency define the four subunits of a novel clathrin AP-like complex. *EMBO J.* **16**, 4194-4204. doi:10.1093/emboj/16.14.4194

Pasula, S., Cai, X., Dong, Y., Messa, M., McManus, J., Chang, B., Liu, X., Zhu, H., Mansat, R. S., Yoon, S.-J. et al. (2012). Endothelial epsin deficiency decreases tumor growth by enhancing VEGF signaling. *J. Clin. Invest.* **122**, 4424-4438. doi:10.1172/JCI64537

Polo, S. and Di Fiore, P. P. (2008). Finding the right partner: science or ART? *Cell* **135**, 590-592. doi:10.1016/j.cell.2008.10.032

Prosser, D. C., Pannunzio, A. E., Brodsky, J. L., Thorner, J., Wendland, B. and O'Donnell, A. F. (2015). alpha-Arrestins participate in cargo selection for both clathrin-independent and clathrin-mediated endocytosis. *J. Cell Sci.* **128**, 4220-4234. doi:10.1242/jcs.175372

Rahman, H. NA., Wu, H., Dong, Y., Pasula, S., Wen, A., Sun, Y., Brophy, M. L., Tessneer, K. L., Cai, X., McManus, J. et al. (2016). Selective targeting of a novel epsin-VEGFR2 interaction promotes VEGF-mediated angiogenesis. *Circ. Res.* **118**, 957-969. doi:10.1161/CIRCRESAHA.115.307679

Rappsilber, J., Mann, M. and Ishihama, Y. (2007). Protocol for micro-purification, enrichment, pre-fractionation and storage of peptides for proteomics using StageTips. *Nat. Protoc.* **2**, 1896-1906. doi:10.1038/nprot.2007.261

Rohrer, J., Bénédetti, H., Zanolari, B. and Riezman, H. (1993). Identification of a novel sequence mediating regulated endocytosis of the G protein-coupled alpha-pheromone receptor in yeast. *Mol. Biol. Cell* **4**, 511-521. doi:10.1091/mbc.4.5.511

Roth, A. F. and Davis, N. G. (1996). Ubiquitination of the yeast a-factor receptor. *J. Cell Biol.* **134**, 661-674. doi:10.1083/jcb.134.3.661

Roth, A. F. and Davis, N. G. (2000). Ubiquitination of the PEST-like endocytosis signal of the yeast a-factor receptor. *J. Biol. Chem.* **275**, 8143-8153. doi:10.1074/jbc.275.11.8143

Roth, A. F., Sullivan, D. M. and Davis, N. G. (1998). A large PEST-like sequence directs the ubiquitination, endocytosis, and vacuolar degradation of the yeast a-factor receptor. *J. Cell Biol.* **142**, 949-961. doi:10.1083/jcb.142.4.949

Rotin, D., Staub, O. and Haguenauer-Tsapis, R. (2000). Ubiquitination and endocytosis of plasma membrane proteins: role of Nedd4/Rsp5p family of ubiquitin-protein ligases. *J. Membr. Biol.* **176**, 1-17. doi:10.1007/s00232001079

Ruiz, A. and Ariño, J. (2007). Function and regulation of the Saccharomyces cerevisiae ENA sodium ATPase system. *Eukaryot. Cell* **6**, 2175-2183. doi:10.1128/EC.00337-07

Sen, A., Madhivanan, K., Mukherjee, D. and Aguilar, R. C. (2012). The epsin protein family: coordinators of endocytosis and signaling. *Biomol. Concepts* **3**, 117-126. doi:10.1515/bmc-2011-0060

Serrano, R., Mulet, J. M., Rios, G., Marquez, J. A., de Larrinoa, I. F., Leube, M. P., Mendizabal, I., Pascual-Ahuir, A., Proft, M., Ros, R. et al. (1999). A glimpse of the mechanisms of ion homeostasis during salt stress. *J. Exp. Bot.* **50**, 1023-1036. doi:10.1093/jxb/50.Special_Issue.1023

Shih, S. C., Katzmann, D. J., Schnell, J. D., Sutanto, M., Emr, S. D. and Hicke, L. (2002). Epsins and Vps27p/Hrs contain ubiquitin-binding domains that function in receptor endocytosis. *Nat. Cell Biol.* **4**, 389-393. doi:10.1038/ncb790

Sigismund, S., Woelk, T., Puri, C., Maspero, E., Tacchetti, C., Transidico, P., Di Fiore, P. P. and Polo, S. (2005). Clathrin-independent endocytosis of ubiquitinated cargos. *Proc. Natl. Acad. Sci. USA* **102**, 2760-2765. doi:10.1073/pnas.0409817102

Soetens, O., De Craene, J.-O. and André, B. (2001). Ubiquitin is required for sorting to the vacuole of the yeast general amino acid permease, Gap1. *J. Biol. Chem.* **276**, 43949-43957. doi:10.1074/jbc.M102945200

Sorkina, T., Miranda, M., Dionne, K. R., Hoover, B. R., Zahniser, N. R. and Sorkin, A. (2006). RNA interference screen reveals an essential role of Nedd4-2 in dopamine transporter ubiquitination and endocytosis. *J. Neurosci.* **26**, 8195-8205. doi:10.1523/JNEUROSCI.1301-06.2006

Staruschenko, A., Pochynyuk, O. and Stockand, J. D. (2005). Regulation of epithelial Na+ channel activity by conserved serine/threonine switches within sorting signals. *J. Biol. Chem.* **280**, 39161-39167. doi:10.1074/jbc.M509608200

Stawiecka-Mirota, M., Pokrzywa, W., Morvan, J., Zoladek, T., Haguenauer-Tsapis, R., Urban-Grimal, D. and Morsomme, P. (2007). Targeting of Sna3p to the endosomal pathway depends on its interaction with Rsp5p and multivesicular body sorting on its ubiquitylation. *Traffic* **8**, 1280-1296. doi:10.1111/j.1600-0854.2007.00610.x

Stimpson, H. E. M., Lewis, M. J. and Pelham, H. R. B. (2006). Transferrin receptor-like proteins control the degradation of a yeast metal transporter. *EMBO J.* **25**, 662-672. doi:10.1038/sj.emboj.7600984

Sugiyama, S., Kishida, S., Chayama, K., Koyama, S. and Kikuchi, A. (2005). Ubiquitin-interacting motifs of Epsin are involved in the regulation of insulin-dependent endocytosis. *J. Biochem.* **137**, 355-364. doi:10.1093/jb/mvi044

Sullivan, J. A., Lewis, M. J., Nikko, E. and Pelham, H. R. B. (2007a). Multiple interactions drive adaptor-mediated recruitment of the ubiquitin ligase rsp5 to membrane proteins in vivo and in vitro. *Mol. Biol. Cell* **18**, 2429-2440. doi:10.1091/mbc.e07-01-0011

Taylor, J. R. (1997). *An Introduction to Error Analysis: The Study of Uncertainties in Physical Measurements*, 2nd edn.: University Science Books.

Tian, X., Hansen, D., Schedl, T. and Skeath, J. B. (2004). Epsin potentiates Notch pathway activity in Drosophila and C. elegans. *Development* **131**, 5807-5815. doi:10.1242/dev.01459

Traub, L. M. and Bonifacino, J. S. (2013). Cargo recognition in clathrin-mediated endocytosis. *Cold Spring Harbor Perspect. Biol.* **5**, a016790. doi:10.1101/cshperspect.a016790

Traub, L. M. and Lukacs, G. L. (2007). Decoding ubiquitin sorting signals for clathrin-dependent endocytosis by CLASPs. *J. Cell Sci.* **120**, 543-553. doi:10.1242/jcs.03385

Wadskog, I., Forsmark, A., Rossi, G., Konopka, C., Öyen, M., Goksör, M., Ronne, H., Brennwald, P. and Adler, L. (2006). The yeast tumor suppressor homologue Sro7p is required for targeting of the sodium pumping ATPase to the cell surface. *Mol. Biol. Cell* **17**, 4988-5003. doi:10.1091/mbc.e05-08-0798

Wang, W. and Struhl, G. (2004). Drosophila Epsin mediates a select endocytic pathway that DSL ligands must enter to activate Notch. *Development* **131**, 5367-5380. doi:10.1242/dev.01413

Wang, W. and Struhl, G. (2005). Distinct roles for Mind bomb, Neuralized and Epsin in mediating DSL endocytosis and signaling in Drosophila. *Development* **132**, 2883-2894. doi:10.1242/dev.01860

Wang, H., Traub, L. M., Weixel, K. M., Hawryluk, M. J., Shah, N., Edinger, R. S., Perry, C. J., Kester, L., Butterworth, M. B., Peters, K. W. et al. (2006). Clathrin-mediated endocytosis of the epithelial sodium channel. Role of epsin. *J. Biol. Chem.* **281**, 14129-14135. doi:10.1074/jbc.M512511200

Wieland, J., Nitsche, A. M., Strayle, J., Steiner, H. and Rudolph, H. K. (1995). The PMR2 gene cluster encodes functionally distinct isoforms of a putative Na+ pump in the yeast plasma membrane. *EMBO J.* **14**, 3870-3882. doi:10.1002/j.1460-2075.1995.tb00059.x

Yenush, L. (2016). Potassium and Sodium Transport in Yeast. *Adv. Exp. Med. Biol.* **892**, 187-228. doi:10.1007/978-3-319-25304-6_8

Supplemental Information

Table SI

Ena1 ST-patch phosphopeptides identified by mass spectrometry

Phospho-Ser/Thr peptide sequences[a]	$[M+H]^+$ (Da)	Percolator q-value
AHNPENDLESNNKRDPFEAY**pS**T**pS**TTIHTEVNIGIK	4181.794576	0.01301
AHNPENDLESNNKRDPFEAYSTST**pT**IH**pT**EVNIGIK	4181.809713	0.006411
a: pS or pT in bold indicate identified phospho-serine and phospho-threonine residues, respectively.		

Table SII: Plasmids used in this study

Name	Description	Source
pUG35 Ena1-GFP	*MET25::ENA1::YEGFP*[a] *CEN URA3*	(Wadskog et al., 2006)
pJLU34 (Ste3-GFP)	*STE3::GFP CEN URA3*	(Urbanowski and Piper, 2001)
Ena1-GFP (*LEU2*)	*MET25::ENA1::YEGFP CEN LEU2*	This study
Ent1.317	*ENT1 CEN LYS2*	Wendland lab, JHU
Ent1.317-3xHA	*ENT1::HAx3 CEN LYS2*	This study
ENTH1.317-3xHA	*ENT1*$^{1\text{-}154}$*::HAx3 CEN LYS2*	This study
Ent1^{Um}.317-3xHA	*ENT1*$^{S177D\ S201D}$*::HA*x3 *CEN LYS2*	This study
ENTH1.317	*ENT1*$^{1\text{-}154}$*CEN LYS2*	This study
ΔENTH1.317	*ENT1*$^{145\text{-}454}$*CEN LYS2*	This study
Ent1^{Um}.317	*ENT1*$^{S177D\ S201D}$ *CEN LYS2*	This study
Ent1$^{1\text{-}235}$.317	*ENT1*$^{1\text{-}235}$*::HA*x3 *CEN LYS2*	This study
Ent2.317	*ENT2 CEN LYS2*	Wendlandlab,JHU
ΔENTH2.317	*ENT2*$^{148\text{-}613}$*CEN LYS2*	This study
Ent2^{Um} .317	*ENT2*$^{S187D\ S218D}$ *CEN LYS2*	This study
Ena1$^{1\text{-}1071}$ -GFP	*MET25::ENA1*$^{\Delta(1072\text{-}1091)}$*::YEGFP CEN URA3*	This study
Ena1$^{1\text{-}1075}$ -GFP	*MET25::ENA1*$^{\Delta(1076\text{-}1091)}$*::YEGFP CEN URA3*	This study
Ena1$^{1\text{-}1079}$ -GFP	*MET25::ENA1*$^{\Delta(1080\text{-}1091)}$*::YEGFP CEN URA3*	This study
Ena1$^{1\text{-}1083}$ -GFP	*MET25::ENA1*$^{\Delta(1084\text{-}1091)}$*::YEGFP CEN URA3*	This study
Ena1$^{1\text{-}1087}$ -GFP	*MET25::ENA1*$^{\Delta(1088\text{-}1091)}$*::YEGFP CEN URA3*	This study
Ena1^{G1088A} -GFP	*MET25::ENA1* ^{G1088A} *::YEGFP CEN URA3*	This study
Ena1^{I1089A} -GFP	*MET25::ENA1* ^{I1089A} *::YEGFP CEN URA3*	This study
Ena1^{Q1091A} -GFP	*MET25::ENA1* ^{Q1091A} *::YEGFP CEN URA3*	This study
Ena1^{K1090R} -GFP	*MET25::ENA1* ^{K1090R} *::YEGFP CEN URA3*	This study
Ena1^{K1090R} -Ub –GFP	*MET25::ENA1* ^{K1090R} - Ub$^{\Delta G75,\ \Delta G76}$*::YEGFP CEN URA3* [b]	This study
Ena1$^{(1088\text{-}1091)G}$ -GFP	*MET25::ENA1* $^{I1089G\ K1090G\ Q1091G}$*::YEGFP CEN URA3*	This study
Ena1$^{(1084\text{-}1087)G}$ -GFP	*MET25::ENA1* $^{E1084G\ V1085G\ N1086GI1087G}$*::YEGFP CEN URA3*	This study
Ena1$^{(1080\text{-}1083)G}$ -GFP	*MET25::ENA1* $^{T1080G\ I1081G\ H1082G\ T1083G}$*::YEGFP CEN URA3*	This study
Ena1$^{(1076\text{-}1079)G}$ -GFP	*MET25::ENA1* $^{S1076G\ T1077GS1078G\ T1079G}$*::YEGFP CEN URA3*	This study
Ena1$^{(1072\text{-}1075)G}$ -GFP	*MET25::ENA1* $^{F1072G\ E1073GA1074G\ Y1075G}$*::YEGFP CEN URA3*	This study
Ena1^{TSTSS} -GFP	*MET25::ENA1* $^{S1076T\ T1077S\ S1078T\ T1079S\ T1080S}$ *::YEGFP CEN URA3*	This study
Ena1^{DGGG} -GFP	*MET25::ENA1* $^{S1076D\ T1077GS1078G\ T1079G}$*::YEGFP CEN URA3*	This study
Ena1^{GDGG} -GFP	*MET25::ENA1* $^{S1076G\ T1077DS1078G\ T1079G}$*::YEGFP CEN URA3*	This study
Ena1^{GGDG} -GFP	*MET25::ENA1* $^{S1076G\ T1077GS1078D\ T1079G}$*::YEGFP CEN URA3*	This study
Ena1^{GGGD} -GFP	*MET25::ENA1* $^{S1076G\ T1077GS1078G\ T1079D}$*::YEGFP CEN URA3*	This study
Ena1^{DDGG} -GFP	*MET25::ENA1* $^{S1076D\ T1077DS1078G\ T1079G}$*::YEGFP CEN URA3*	This study
Ena1^{DGDG} -GFP	*MET25::ENA1* $^{S1076D\ T1077GS1078D\ T1079G}$*::YEGFP CEN URA3*	This study
Ena1^{DGGD} -GFP	*MET25::ENA1* $^{S1076D\ T1077GS1078G\ T1079D}$*::YEGFP CEN URA3*	This study
Ena1^{GDDG} -GFP	*MET25::ENA1* $^{S1076G\ T1077DS1078D\ T1079G}$*::YEGFP CEN URA3*	This study
Ena1^{GDGD} -GFP	*MET25::ENA1* $^{S1076G\ T1077DS1078G\ T1079D}$*::YEGFP CEN URA3*	This study
Ena1^{GGDD} -GFP	*MET25::ENA1* $^{S1076G\ T1077GS1078D\ T1079D}$*::YEGFP CEN URA3*	This study
Ena1^{AAST} -GFP	*MET25::ENA1* $^{S1076A\ T1077A}$*::YEGFP CEN URA3*	This study
Ena1^{ATAT} -GFP	*MET25::ENA1* $^{S1076A\ S1078A}$ *::YEGFP CEN URA3*	This study

Ena1^{ATSA} -GFP	*MET25::ENA1* $^{S1076A\ T1079A}$ *::YEGFP CEN URA3*	This study
Ena1^{SAAT} -GFP	*MET25::ENA1* $^{T1077A\ S1078A}$ *::YEGFP CEN URA3*	This study
Ena1^{SASA} -GFP	*MET25::ENA1* $^{T1077A\ T1079A}$ *::YEGFP CEN URA3*	This study
Ena1^{STAA} -GFP	*MET25::ENA1* $^{S1078A\ T1079A}$ *::YEGFP CEN URA3*	This study
Ena1^{ATST} -GFP	*MET25::ENA1* ^{S1076A} *::YEGFP CEN URA3*	This study
Ena1^{DDST} -GFP	*MET25::ENA1*$^{S1076D\ T1077D}$*::YEGFP CEN URA3*	This study
Ena1^{AAST} -Ub -GFP	*MET25::ENA1*$^{S1076A\ S1077A}$ - Ub$^{\Delta G75,\ \Delta G76}$ *::YEGFP CEN URA3* [a]	This study
Ena1$^{DDST,\ K1090R}$ -GFP	*MET25::ENA1*$^{S1076D\ T1077D\ K1090R}$*::YEGFP CEN URA3*	This study
Ena1$^{DDST,\ K1090R}$- Ub-GFP	*MET25::ENA1*$^{S1076D\ T1077D\ K1090R}$-Ub$^{,\Delta G75,\ \Delta G76)}$ *::YEGFP CEN URA3*[a]	This study
Ena1^{TDTT} -GFP	*MET25::ENA1* $^{S1076T\ T1077D\ S1078T}$*::YEGFP CEN URA3*	This study
Ena1^{ETET} -GFP	*MET25::ENA1*$^{S1076E\ S1078E}$*::YEGFP CEN URA3*	This study
Ena1$^{dupl(1066-1070)}$ -GFP	*MET25::ENA1::YEGFP* with N^{1066}NRRD^{1070} duplicated *CEN URA3*	This study
Ena1 $^{dupl(1081-1085)}$ -GFP	*MET25::ENA1::YEGFP* with I^{1081}HTEV^{1085}duplicated *CEN URA3*	This study
Ena1$^{\Delta(1083-1087)}$ -GFP	*MET25::ENA1*$^{\Delta(1083-1087)}$*::YEGFP CEN URA3*	This study
Ena1$^{\Delta(1058-1091)}$-GFP	*MET25::ENA1*$^{\Delta(1058-1091)\ )}$*::YEGFP CEN URA3*	This study
Ena1^{K1090R}-pHluorin	*MET25::* Ena1^{K1090R}*::pHluorin CEN URA3*	This study
Ena1^{K1090R}-Ub-pHluorin	*MET25::* Ena1^{K1090R}-Ub$^{\Delta G75,\ \Delta G76}$*::pHluorin CEN URA3*	This study
GFP-Tre1	*TPI1::GFP::TRE1* in Ycplac33, *CEN URA3*	(Stimpson et al., 2006)
pLJ721(Yck1)	*YCK1 2μ URA3*	(Robinson et al., 1992)
pLS2.3 (Yck2)	*YCK2 2μ URA3*	(Robinson et al., 1992)
Yck1-His$_6$	*GAL10::YCK1$^{1-536}$-His$_6$ 2μ URA3*	This study
Yck2-His$_6$	*GAL1::YCK1$^{1-546}$-His$_6$ 2μ URA3*	This study
Art3. 425	*ART3 2μ, LEU2*	(O'Donnell et al., 2010)
HA-ΔENTH1. 426	*MET25::HAx3::ENT1$^{149-454}$ 2μ, URA3*	This study
HA-ΔENTH1. 317	*ENT1$^{149-454}$ ::HAx3 CEN LYS2*	This study
His$_6$-Ent1	pET28a His$_6$-Ent1	(Aguilar et al., 2003)
His$_6$-Ent2	pET28c His$_6$-Ent2	Lab collection
Ub-GST	pET3a Ub-GST	kindly provided by the late Cecile Pickart (Johns Hopkins)
Ena1^{K1090R} -Ub-GST	pET3a Ena1$^{1076-1091,K1090R}$ - Ub-GST	This study
DDST-Ub-GST	pET3a Ena1$^{1076-1091,\ S1076DT,\ 1077D}$ - Ub-GST	This study
GST	pGEX-4T-1	Lab collection
pRS 425	*2μ, LEU2*	(Sikorski and Hieter, 1989)
pRS 317	*CEN, LYS*	Lab collection
pRS 426	*2μ, URA3*	Lab collection

a: Enhanced Green Fluorescence Protein with yeast codon optimization.

b: The ubiquitin moiety fused to the constructs was Ub$^{K48R,\Delta G75,\Delta G76}$, where K48R prevents formation of K48 linked polyubiquitin chains that have been reported to primarily signal degradation (Pickart and Fushman, 2004), and elimination of two C- terminal glycine residues prevents recognition and cleavage by deubiquitinating enzymes (Drag et al., 2008).

Table SIII: Strains used in this study

Name	Description	Source
SEY6210	*MAT***a** *leu2-3,112 ura3-52 his3-200 trp1-901 lys2-801 suc2-9*	Laboratory strain
W303	*MAT***α** *ade2-1 his3-1 leu2-3112 trp1-1 ura3-1 can1-100*	Laboratory strain
BY4741	*MAT***a** *his3*Δ1 *leu2*Δ0 *LYS2 met15*Δ0 *ura3*Δ0	Laboratory strain
BY4742	*MATα his3Δ1 leu2Δ0 lys2Δ0 ura3Δ0*	Laboratory strain
ent1Δent2Δ[a]	*MAT***a** *ent1::HIS3 ent2::HIS3* in SEY6210	(Aguilar et al., 2006)
ent1Δ	*MAT***a** *ent1::KANMX* in SEY6210	Laboratory collection
ent2Δ	*MAT***a** *ent2::KANMX* in SEY6210	Laboratory collection
sla2Δ	*MAT*α *sla2:: HisMX* in SEY6210	(Stefan et al., 2005)
LRB756(*yck1Δ yck2ts*)	*MAT***a** *his3 leu2 ura3-52 yck1-Δ1::ura3 yck2-2ts*	(Panek et al., 1997)
LRB758 WT	*MAT***a** *his3 leu2 ura3-52*	(Panek et al., 1997)
ypk1Δ	*MAT***a** *his3Δ1 leu2Δ0 met15Δ0 ura3Δ0 ypk1::KanMX*	*MAT***a** deletion collection
ypk2Δ	*MAT***a** *his3Δ1 leu2Δ0 met15Δ0 ura3Δ0 ypk2::KanMX*	*MAT***a** deletion collection
pkh1Δ	*MAT***a** *his3Δ1 leu2Δ0 met15Δ0 ura3Δ0 pkh1::KanMX*	*MAT***a** deletion collection
pkh2Δ	*MAT***a** *his3Δ1 leu2Δ0 met15Δ0 ura3Δ0 pkh2::KanMX*	*MAT***a** deletion collection
ptk2Δ	*MAT***a** *his3Δ1 leu2Δ0 met15Δ0 ura3Δ0 ptk2::KanMX*	*MAT***a** deletion collection
kkq8Δ	*MATa his3Δ1 leu2Δ0 met15Δ0 ura3Δ0 kkq8::KanMX*	*MAT***a** deletion collection
INA 17-4D	*ura3 leu2 trp1 his2 ade1*	(Inagaki et al., 1999)
INA 106-3B	$pkh1^{D398G}$ *pkh2Δ::LEU2*	(Inagaki et al., 1999)
art1Δ	*MATα his3Δ1 leu2Δ0 lys2Δ0 ura3Δ0 art1::KanMX*	*MAT*α deletion collection
art2Δ	*MATα his3Δ1 leu2Δ0 lys2Δ0 ura3Δ0 art2::KanMX*	*MAT*α deletion collection

art3Δ	*MATα his3Δ1 leu2Δ0 lys2Δ0 ura3Δ0 art3::KanMX*	*MAT*α deletion collection
art4Δ	*MATα his3Δ1 leu2Δ0 lys2Δ0 ura3Δ0 art4::KanMX*	*MAT*α deletion collection
art5Δ	*MATα his3Δ1 leu2Δ0 lys2Δ0 ura3Δ0 art5::KanMX*	*MAT*α deletion collection
art6Δ	*MATα his3Δ1 leu2Δ0 lys2Δ0 ura3Δ0 art6::KanMX*	*MAT*α deletion collection
art7Δ	*MATα his3Δ1 leu2Δ0 lys2Δ0 ura3Δ0 art7::KanMX*	*MAT*α deletion collection
art8Δ	*MATα his3Δ1 leu2Δ0 lys2Δ0 ura3Δ0 art8::KanMX*	*MAT*α deletion collection
art9Δ	*MATα his3Δ1 leu2Δ0 lys2Δ0 ura3Δ0 art9::KanMX*	*MAT*α deletion collection
art10Δ	*MATα his3Δ1 leu2Δ0 lys2Δ0 ura3Δ0 art10::KanMX*	*MAT*α deletion collection
MAY14	*MATα gga1::TRP1 gga2::HIS3*	*(Abazeed and Fuller, 2008)*
RH4344(rcy1Δ)	*MATa yjl204c::kanMX his4 leu2 ura3 lys2 bar1*	*(Wiederkehr et al., 2000)*
a It should be noted that these cells express the ENTH domain of Ent1 to sustain viability (Aguilar et al., 2006).		

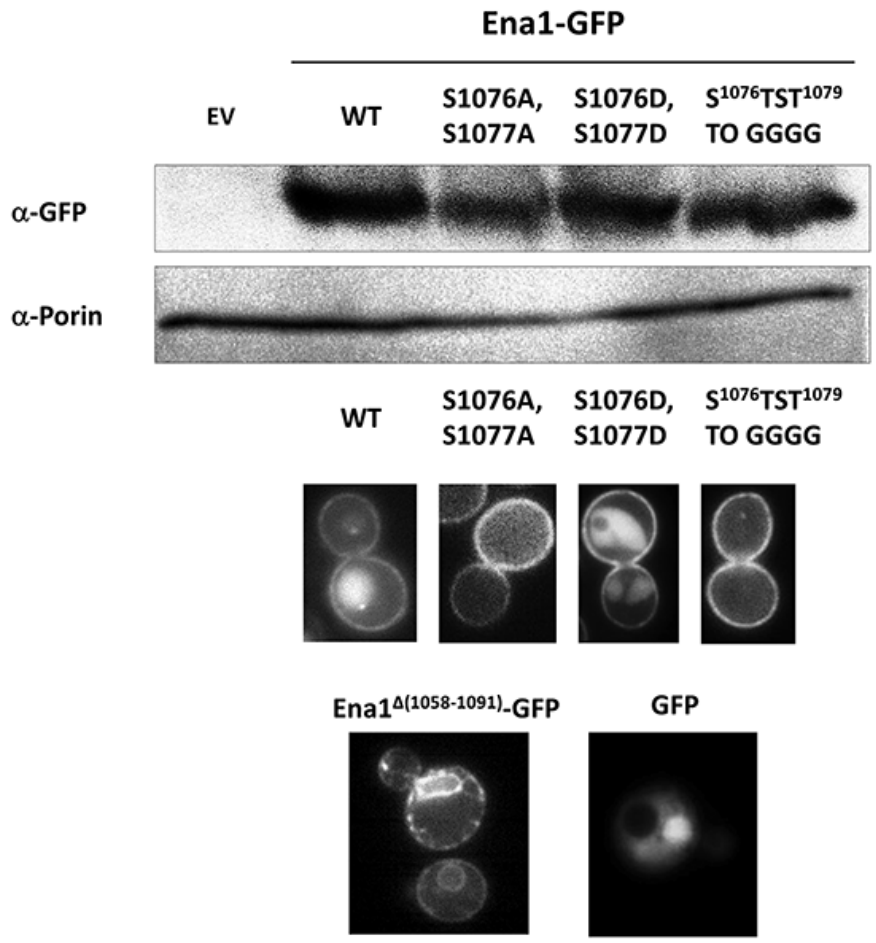

Fig. S1

The stability and expression levels of Ena1-GFP WT or mutants were monitored by Western blotting (upper panel) and the presence/analysis of their intracellular distribution patterns by microscopy (lower panels). Western blotting was conducted as described in *materials and methods* on whole cell lysates from cells transformed with empty vector (EV) and plasmids encoding for Ena1-GFP WT and mutants (only 3 are shown as example). Presence of Ena1-GFP was investigated using an anti-GFP antibody, while the signal from the mitochondrial protein porin was used as loading control. In addition to protein levels, the different Ena1-GFP variants were analyzed/evaluated by their intracellular distribution. Specifically, to be considered for this study, the evaluated proteins were also expected to show a pattern substantially different from plain GFP or typical ER-retention pattern (*e.g.,* Ena1$^{\Delta(1058\text{-}1091)}$).

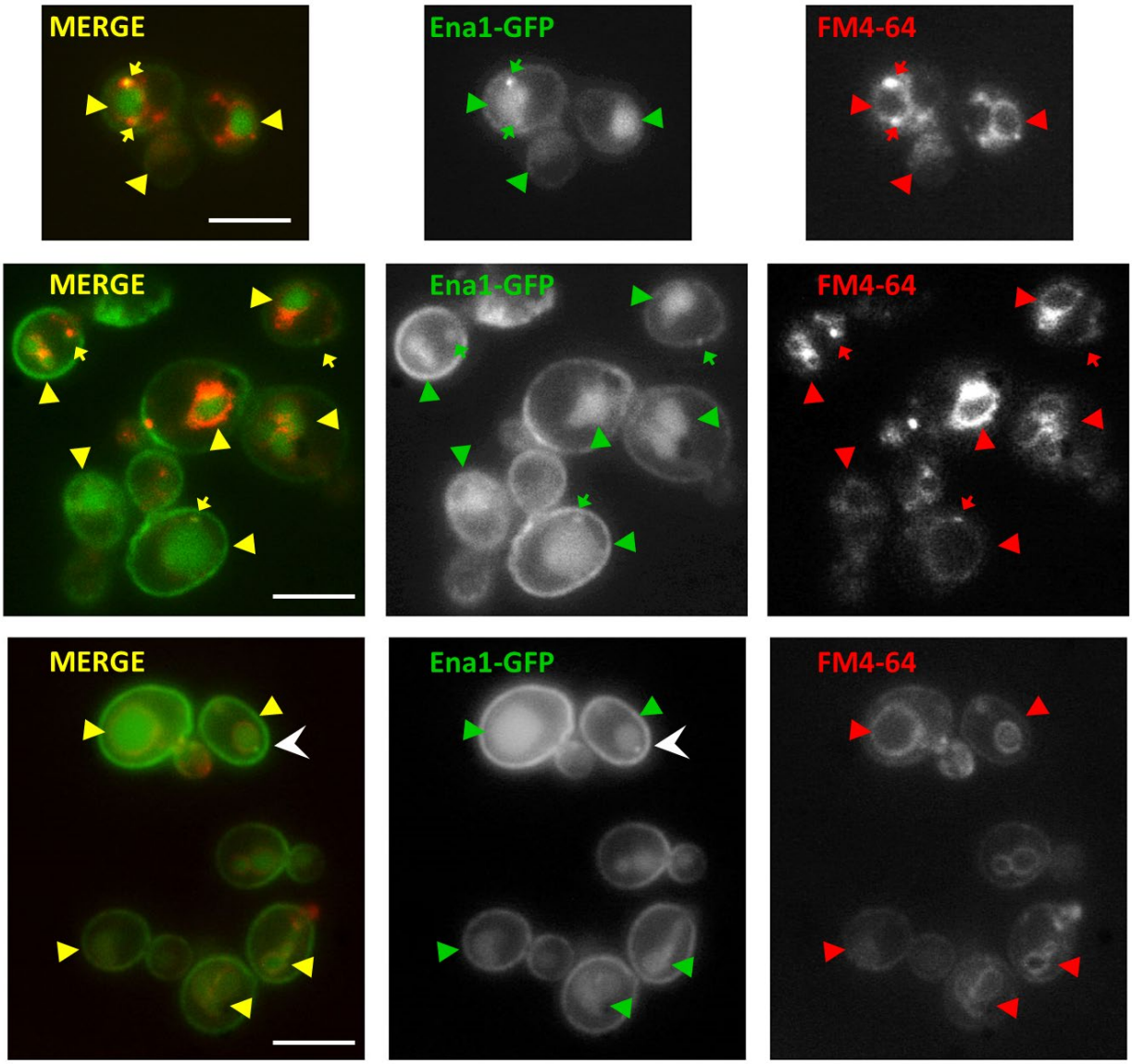

Fig. S2

Cells expressing Ena1-GFP displayed intracellular structures labeled with the lipophilic dye FM4-64 used to mark the endocytic pathway. These Ena1-GFP positive compartments colocalized with FM4-64 (95%) in vacuoles (arrowheads) and punctate structures (arrows). White arrowhead points to one example of the very few Ena1-GFP compartments that do not colocalize with FM4-64; these intracellular structures may represent a secretory compartment.

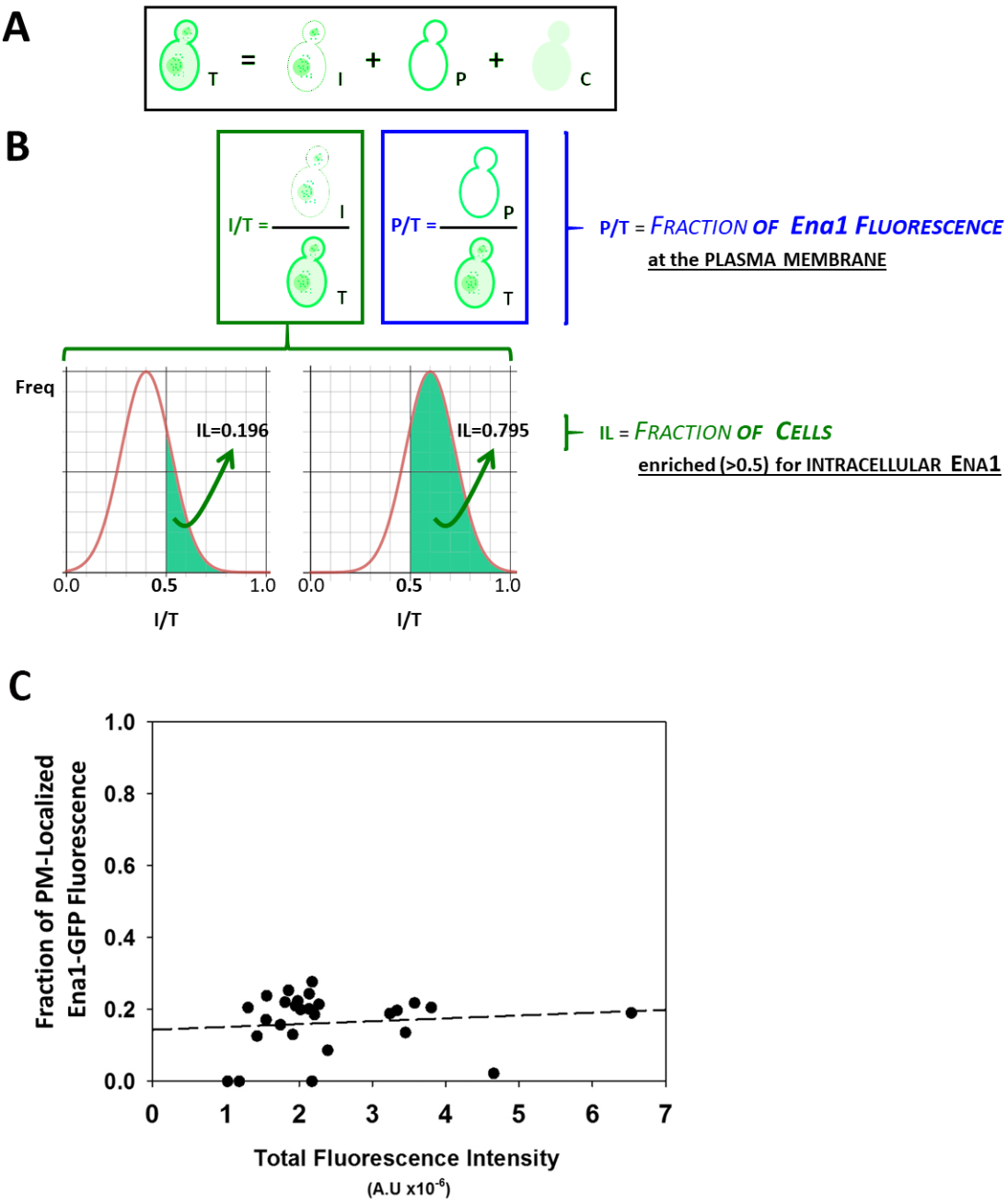

Fig. S3

A. Schematic representation of the contributing fractions (I: internal, P: plasma membrane and C: cytosolic) to the total (T) fluorescence. **B**. While the *P/T ratio* reports the relative amount *GFP-Ena1 fluorescence at the plasma membrane in cells*, the *IL* reflects the *fraction of cells in the population* enriched in intracellular GFP-Ena1. **C**. The fraction of PM-associated (P/T—see *Materials and methods*) Ena1-GFP fluorescence as a function of total

cellular fluorescence intensity. Although P/T values displayed typical biological variability, their median range remained fairly constant only varying between extrapolated values of 0.14 to 0.19 (the latter representing high over-expressors—which were excluded from the current study)

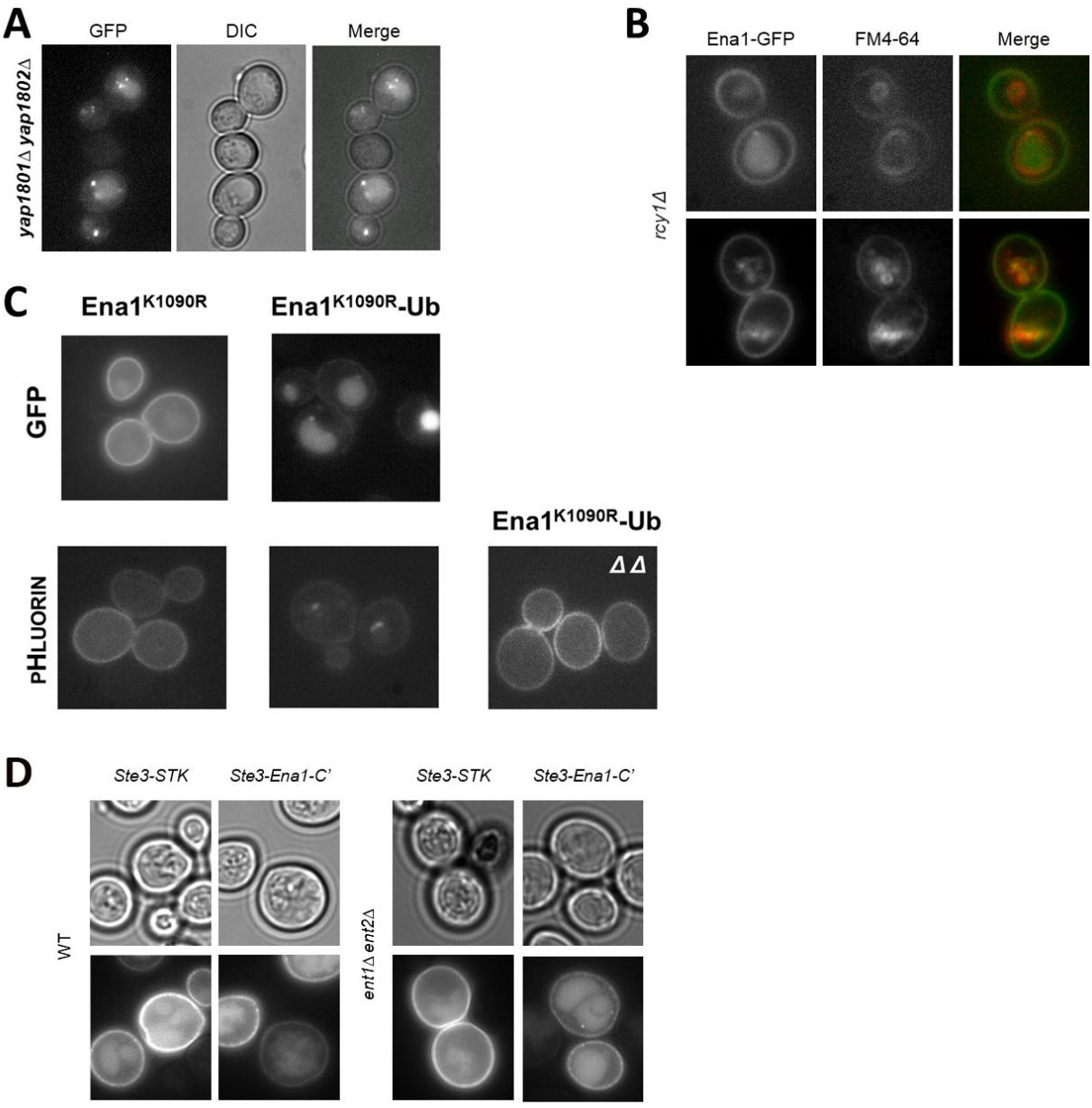

Fig. S4

Different GFP-fusion transmembrane proteins (Ena1: **A**-**C** and Ste3: **D**) variants were expressed in the indicated yeast strains. Representative fluorescent images are included and contrasted to DIC (**A** and **D**) or FM4-64 (**B**) channels.

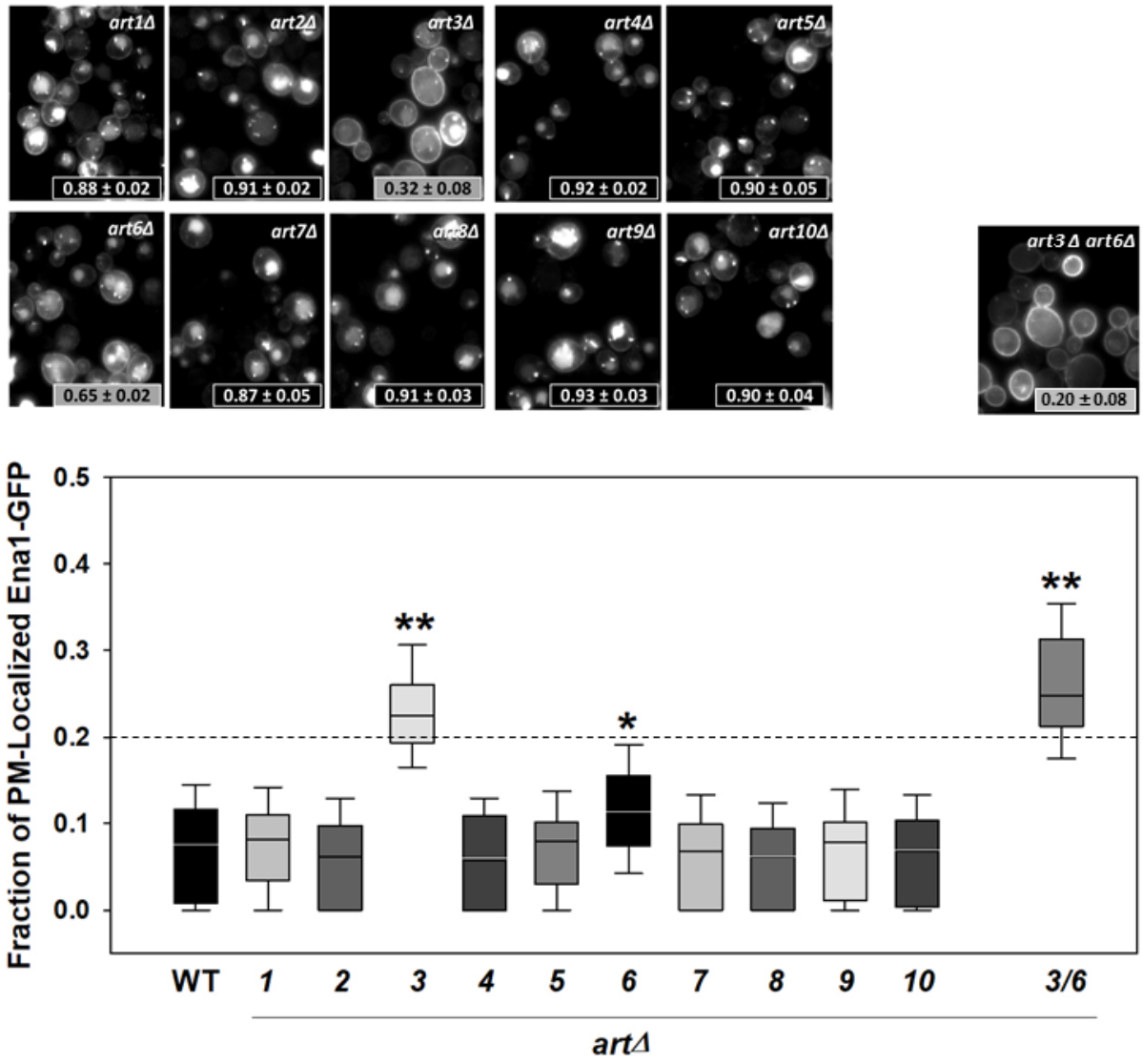

Fig. S5

A complete collection of *ART* single deletes strains in BY4742 background expressing Ena1-GFP were imaged as described in Materials and methods. IL values and relative Ena1-GFP PM accumulation for the indicated strains was estimated and statistically analyzed with respect to the corresponding WT strain as in Fig. 1. **: $p << \alpha_C=0.001$; *: $p < \alpha_C=0.001$—Wilcoxon's test.

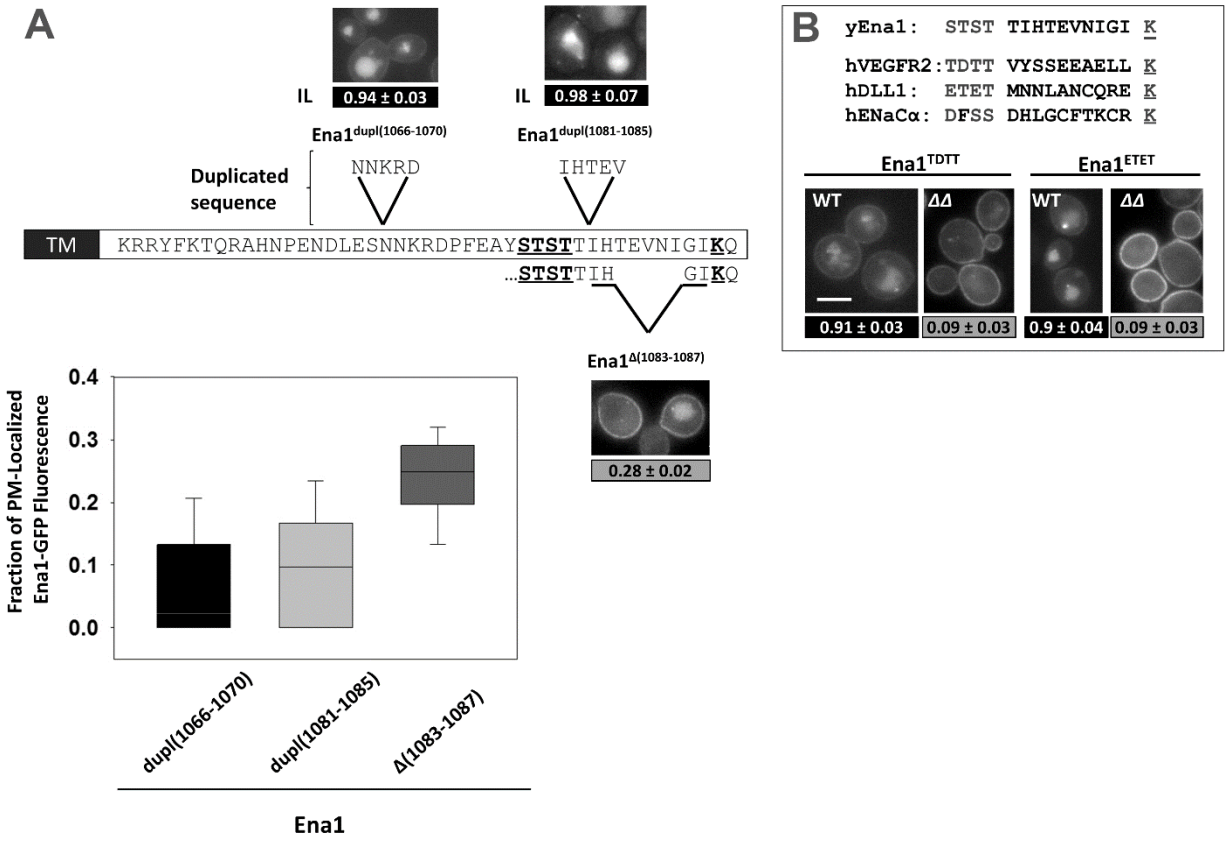

Fig. S6

A. The indicated Ena1-GFP mutants were expressed in yeast cells and IL indexes and relative PM accumulation values were estimated as in Fig. 1. Representative images are included. **B.** *Upper panel*: Alignment shows “STK”-like sequences (with conserved spacing from the transmembrane domain and among the ST-patch to K distance) from known mammalian epsin cargoes as compared to yeast Ena1. Chimeric proteins were created replacing Ena1 WT $S^{1076}TST^{1079}$ sequence for the hVEGFR2 TDTT ($Ena1^{TDTT}$) and hDLL1 ETET ($Ena1^{ETET}$) that in conjunction with K^{1090} recreated the mammalian STK motifs. y: yeast; h: human. *Lower panel*: Intracellular localization of $Ena1^{TDTT}$-GFP (left) and $Ena1^{ETET}$ (right) was analyzed in WT and ΔΔ cells. IL indexes were estimated and analyzed as described in Fig. 1. Representative images are also included. Scale bar: 5μm.

References for supplemental information

ABAZEED, M. E. & FULLER, R. S. 2008. Yeast Golgi-localized, gamma-Ear-containing, ADP-ribosylation factor-binding proteins are but adaptor protein-1 is not required for cell-free transport of membrane proteins from the trans-Golgi network to the prevacuolar compartment. *Mol Biol Cell,* 19**,** 4826-36.

AGUILAR, R. C., LONGHI, S. A., SHAW, J. D., YEH, L. Y., KIM, S., SCHON, A., FREIRE, E., HSU, A., MCCORMICK, W. K., WATSON, H. A. & WENDLAND, B. 2006. Epsin N-terminal homology domains perform an essential function regulating Cdc42 through binding Cdc42 GTPase-activating proteins. *Proceedings of the National Academy of Sciences of the United States of America,* 103**,** 4116-4121.

AGUILAR, R. C., WATSON, H. A. & WENDLAND, B. 2003. The yeast Epsin Ent1 is recruited to membranes through multiple independent interactions. *J Biol Chem,* 278**,** 10737-43.

DRAG, M., MIKOLAJCZYK, J., BEKES, M., REYES-TURCU, F. E., ELLMAN, J. A., WILKINSON, K. D. & SALVESEN, G. S. 2008. Positional-scanning fluorigenic substrate libraries reveal unexpected specificity determinants of DUBs (deubiquitinating enzymes). *Biochem J,* 415**,** 367-75.

INAGAKI, M., SCHMELZLE, T., YAMAGUCHI, K., IRIE, K., HALL, M. N. & MATSUMOTO, K. 1999. PDK1 homologs activate the Pkc1-mitogen-activated protein kinase pathway in yeast. *Mol Cell Biol,* 19**,** 8344-52.

O'DONNELL, A. F., APFFEL, A., GARDNER, R. G. & CYERT, M. S. 2010. Alpha-arrestins Aly1 and Aly2 regulate intracellular trafficking in response to nutrient signaling. *Molecular biology of the cell,* 21**,** 3552-66.

PANEK, H. R., STEPP, J. D., ENGLE, H. M., MARKS, K. M., TAN, P. K., LEMMON, S. K. & ROBINSON, L. C. 1997. Suppressors of YCK-encoded yeast casein kinase 1 deficiency define the four subunits of a novel clathrin AP-like complex. *EMBO J,* 16**,** 4194-204.

PICKART, C. M. & FUSHMAN, D. 2004. Polyubiquitin chains: polymeric protein signals. *Curr Opin Chem Biol,* 8**,** 610-6.

ROBINSON, L. C., HUBBARD, E. J., GRAVES, P. R., DEPAOLI-ROACH, A. A., ROACH, P. J., KUNG, C., HAAS, D. W., HAGEDORN, C. H., GOEBL, M. & CULBERTSON, M. R. 1992. Yeast casein kinase I homologues: an essential gene pair. *Proc Natl Acad Sci U S A,* 89**,** 28-32.

SIKORSKI, R. S. & HIETER, P. 1989. A system of shuttle vectors and yeast host strains designed for efficient manipulation of DNA in Saccharomyces cerevisiae. *Genetics,* 122**,** 19-27.

STEFAN, C. J., PADILLA, S. M., AUDHYA, A. & EMR, S. D. 2005. The phosphoinositide phosphatase Sjl2 is recruited to cortical actin patches in the control of vesicle formation and fission during endocytosis. *Mol Cell Biol,* 25**,** 2910-23.

STIMPSON, H. E., LEWIS, M. J. & PELHAM, H. R. 2006. Transferrin receptor-like proteins control the degradation of a yeast metal transporter. *EMBO J,* 25**,** 662-72.

URBANOWSKI, J. L. & PIPER, R. C. 2001. Ubiquitin sorts proteins into the intralumenal degradative compartment of the late-endosome/vacuole. *Traffic,* 2**,** 622-30.

WADSKOG, I., FORSMARK, A., ROSSI, G., KONOPKA, C., OYEN, M., GOKSÖR, M., RONNE, H., BRENNWALD, P. & ADLER, L. 2006. The yeast tumor suppressor homologue Sro7p is required for targeting of the sodium pumping ATPase to the cell surface. *Mol Biol Cell,* 17**,** 4988-5003.

WIEDERKEHR, A., AVARO, S., PRESCIANOTTO-BASCHONG, C., HAGUENAUER-TSAPIS, R. & RIEZMAN, H. 2000. The F-box protein Rcy1p is involved in endocytic membrane traffic and recycling out of an early endosome in Saccharomyces cerevisiae. *J Cell Biol,* 149**,** 397-410.